

T-1389

GEOPHONE ARRAY FILTERING

by

Erkin Gokturk

ProQuest Number: 10781734

All rights reserved

INFORMATION TO ALL USERS

The quality of this reproduction is dependent upon the quality of the copy submitted.

In the unlikely event that the author did not send a complete manuscript and there are missing pages, these will be noted. Also, if material had to be removed, a note will indicate the deletion.



ProQuest 10781734

Published by ProQuest LLC (2018). Copyright of the Dissertation is held by the Author.

All rights reserved.

This work is protected against unauthorized copying under Title 17, United States Code
Microform Edition © ProQuest LLC.

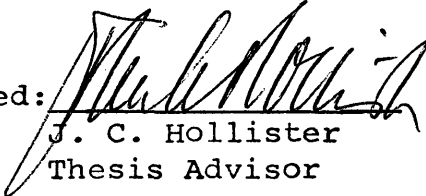
ProQuest LLC.
789 East Eisenhower Parkway
P.O. Box 1346
Ann Arbor, MI 48106 – 1346

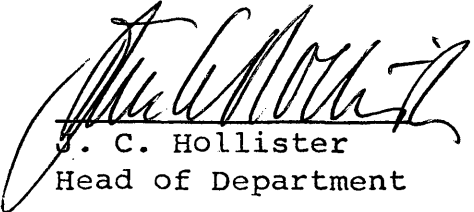
A Thesis submitted to the Faculty and the Board of Trustees of the Colorado School of Mines in partial fulfillment of the requirements for the degree of Master of Science in Geophysical Engineering.

Signed: 
Erkin Gokturk

Golden, Colorado

Date: May 13, 1971

Approved: 
J. C. Hollister
Thesis Advisor


J. C. Hollister
Head of Department

Golden, Colorado

Date: May 13, 1971

ABSTRACT

A geophone array is a collection of identical geophones which are areally distributed in a prescribed fashion. The outputs of the geophones are added to obtain one measured function of time. It is used in problems requiring high resolution. The performance of a geophone array depends upon the number and arrangement of the geophones. Geophone arrays can be considered as wave-length filters.

The response of a geophone array is a function of the wave-length of the incident energy as well as the move-out time across the array. In this study the geophone array responses are presented in two dimensions. The best response of the geophone array is defined as a rectangular response in the wave-number domain. We have chosen the "truncated sinc" arrays which will approximate this desired response.

TABLE OF CONTENTS

	Page
INTRODUCTION	1
BASIC THEORY OF ARRAYS	2
Apparent Velocity and Apparent Wave- number of Harmonic Waves	3
Wave-number Filters	7
Array Shapes	9
COMPUTING RESPONSE OF ARRAYS	11
Inline Arrays	12
Areal Arrays	14
Two-dimensional Theory of Areal Arrays	16
MATHEMATICAL THEORY	18
COMPUTING TWO-DIMENSIONAL RESPONSE OF ARRAYS	26
COMPARISON OF ARRAYS	32
Array A	32
Square Arrays and Array B	37
Square Arrays	37
Array B	37
Array C	43

	Page
Array D	49
Rectangular Arrays	49
Star Arrays	49
CONCLUSIONS	58
REFERENCES	60

ILLUSTRATIONS

Figure /	Page
1. An uptravelling harmonic wave incident to the surface has an apparent wavelength λ_a expressed in feet/cycle	4
2. Array processing	8
3. Five-geophone inline array	12
4. Amplitudes of an equally weighed continuous line of geophones	12
5. Simple nine-geophone two-dimensional array.	16
6. Signal and noise regions	19
7. Ideal low-pass filter	20
8. Continuous line of geophones over length L	21
9. Truncated Sinc function	22
10. Fourier transform of truncated sinc function.	23
11. Nine-geophone array in XY-plane	28
12. Flowchart of the two-dimensional Fourier transform of a geophone array and mapping of the amplitude response	29
13. Deformation of four-geophone array	43
14. Sketch to find amplitude response of deformed array	45

ACKNOWLEDGEMENTS

It is a great pleasure to express my sincere gratitude for the inspiration and the guidance provided to me by Professors John C. Hollister and Frank A. Hadsell during the course of this study. I also thank Professor John R. Hayes of Geology Department for his time.

I would like to thank Türkiye Petrolleri Anonim Ortaklığı for the financial support throughout the graduate study.

To my wife

TÛRKÂN

for her constant encouragement

and patience

INTRODUCTION

The present use of multiple geophone arrays in seismic reflection work represents an effort by the geophysicist to secure usable data in so-called "no reflection" areas. Seismic reflection records in these areas are characterized by noise originating with the shot, and of such a level as to obscure the reflected events. The use of geophone arrays accomplishes two important tasks; cancellation of unwanted energy and improved sampling of the wave-front.

The purpose of the present study was to put the use of multiple geophones on a more scientific footing. We cannot, however, completely reject individual noise waves, but we can choose our "ideal" wave-number response which uniformly passes the signal with zero phase shift and rejects the noise if signal and noise wave-number spectra do not overlap. A Sinc function $(\sin \pi Kx)/\pi x$ transforms into a function $A(K)$ defined by

$$A(K) = \begin{cases} 1 & \text{for } |K| < K_c \\ 0 & \text{for } |K| > K_c \end{cases} ,$$

therefore, transform of the truncated Sinc function in the space domain will approximate the desired rectangular filter response given above. Geophone array response maps were designed according to the above criterion. A method for computing the maps of arrays which were derived from a particular basic array (i.e. square array) by displacement of the geophones will be given later in the study.

Finally, comparisons between some undesirable arrays and the arrays designed with the above criterion are presented.

BASIC THEORY OF ARRAYS

Before discussing the arrays, it is helpful to consider the relationship between "apparent velocity", "move-out per geophone", and "wave-number" of seismic events as recorded on a surface spread of geophones.

Apparent Velocity and Apparent Wave-number of Harmonic Waves

Figure 1 shows a harmonic (sinusoidal) wave propagating upward at an emergent angle θ and at velocity V where successive points of the "wave-front" are shown at three different times. The wave-front is defined for our purpose as a particular nodal plane of the sinusoid. The wave-front is detected by two adjacent geophones g_1 and g_2 whose separation is Δx . The difference in arrival times at g_1 and g_2 ($\Delta t = t_2 - t_1$) is the move-out per geophone spacing. At time t_3 the wave-front has traveled a distance of one wave-length, λ , from its position at time t_1 .

The apparent velocity V_a is the rate at which the wave-front appears to progress along the spread, and is calculated

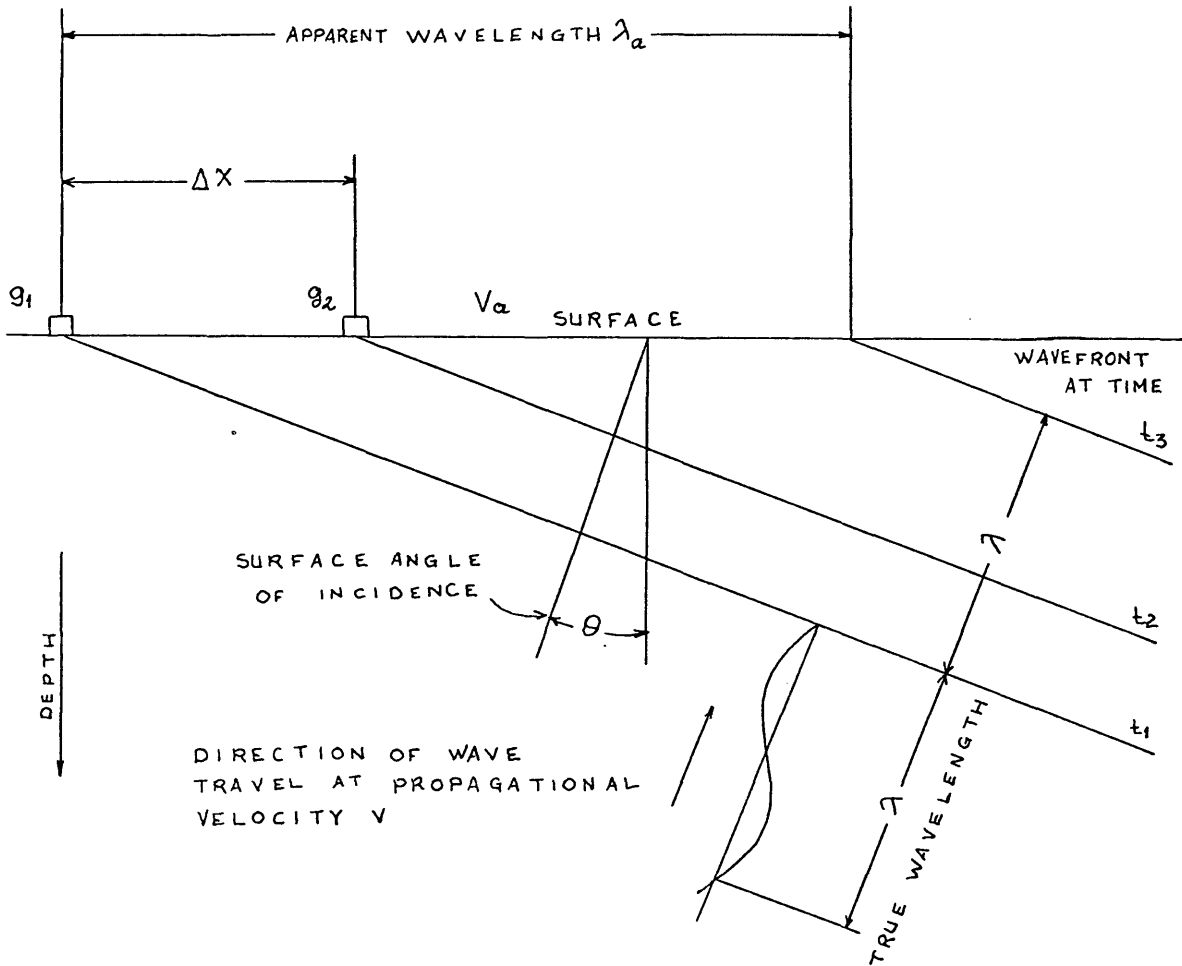


Figure 1. An uptravelling harmonic wave incident to the surface has an apparent wave-length, λ_a , expressed in feet/cycle.

by dividing the spacing ΔX (in feet) by the observed move-out Δt (in seconds). The magnitude of the apparent velocity depends on the propagational velocity and on the surface angle of incidence, $V_a = V/\sin\theta$.

The physical significance of spatial frequency (or wave-number) may be visualized by reference to the positions of the wave-front in Figure 1 at the times t_1 and t_3 . The positions are separated by distance of one true wave-length λ . The apparent wave-length, λ_a , is the horizontal distance subtended along the surface spread by the true wave-length, which corresponds to one cycle of the harmonic wave. The apparent wave-length is evaluated in units of feet per cycle.

The true spatial frequency K is defined to be $1/\lambda$. This is analogous to the temporal frequency f defined to be $1/T$ where T is the period of the oscillation in time. The true temporal frequency f will always be observable on a seismic trace regardless of the direction of propagation of the wave-front. On the other hand, the true spatial frequency K cannot be deduced from a horizontal array of geophones unless the incident angle is known. What we can observe is the apparent wave-length λ_a along the geophone array and define an apparent spatial frequency K_a given by

$$K_a = \frac{1}{\lambda_a} \quad (1)$$

Thus, the propagating wave-front moving toward the surface will appear on the horizontal array as a harmonic wave, travelling in the positive X-direction. Its mathematical expression is $A \cos 2\pi(ft - K_a X)$.

The apparent wave-number K of a harmonic wave of temporal frequency, f , can be calculated in terms of the apparent velocity, which in turn can be expressed in terms of ΔX and Δt . The apparent wave-length λ_a is related to the apparent velocity V_a by the relation $V_a = f \lambda_a$. Since $V_a = \Delta X / \Delta t$, therefore, $\Delta X / \Delta t = f \lambda_a$ from which we will have

$$\frac{1}{\lambda_a} = K_a = f \frac{\Delta t}{\Delta X} \quad \text{cycles per foot (spatial frequency)} \quad (2)$$

Since, $\lambda_a = \lambda / \sin \theta$, then two limiting conditions apply on λ_a are

$$\begin{aligned} \lim_{\theta \rightarrow \pi/2} \lambda_a &= \lambda \\ \lim_{\theta \rightarrow 0} \lambda_a &= \infty \end{aligned} \quad (3)$$

If only the nearly vertical plane waves are considered to contain useful information, the angle of emergence is a

useful means of distinguishing signal from noise. Since, in seismic exploration, deep reflections are signals, from equation (3) it can be shown that wave-numbers for the signal will approach to zero. This permits us to locate the signal in the spatial frequency-domain.

In the remainder of this thesis the only apparent values of the wave-number will be discussed since no knowledge of true propagation wave-numbers will be assumed. For convenience in notation the subscript in λ and K will be dropped but still implied.

Wave-number Filters

Rapid change in apparent wave-length (or apparent velocity) as a function of the angle of emergence affords a means of discriminating against surface waves, direct waves, and refracted waves, all of which contain a dominant horizontal component ($\theta \rightarrow \pi/2$) and may thus be filtered out by means of a suitable array of geophones which is long compared with the wave-length of the undesirable events (Graebner, 1960). On the other hand, reflected harmonic waves which come from greater depths and, therefore, possess a very small angle of emergence are characterized by a very long apparent wave-length. The array length which is to be

constructed must be small in relation to the reflected wavelength, so as not to attenuate it. A field technique designed to meet above requisites is variously known as "wave-length", or "wave-number filtering". Figure 2 shows the mathematical model which describes the array processing, delays τ_n and $\tilde{\tau}_n$ are geophone spacing divided by apparent velocities of signal and noise respectively. Delay between the elements is the time for the energy to travel from one geophone to the other, weights are the gain of the individual geophones and/or the number of geophones effective at the same time while the energy travels along the surface spread of geophones. Summing process represents the connecting

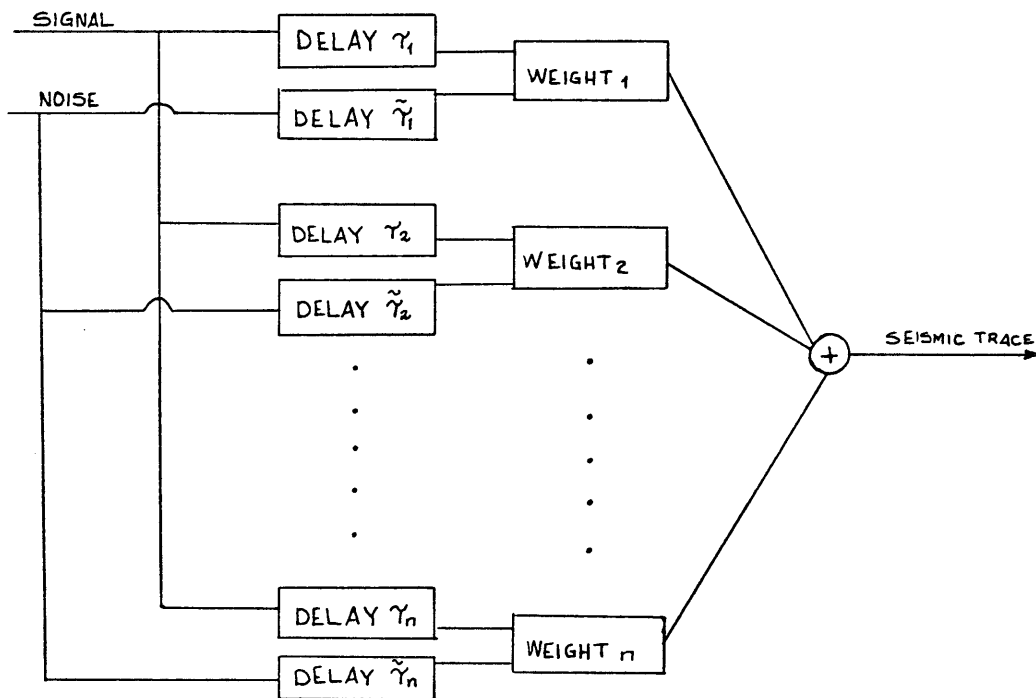


Figure 2. Array processing

the array of geophones into a single channel which represents the seismic trace.

Therefore, we conclude that an array of geophones behaves as a space-domain filter and the use of wave-number filtering permits the recording of a broad frequency range of reflected energies.

Array Shapes

Geophone arrays are used to reject horizontally travelling energy and they serve two important tasks for the improvement of signal to noise ratio. First, they may partially cancel unwanted systematic energy such as ground roll, secondly they may yield a better sampling of an irregular wave-front. The irregularity of the oncoming wave-front may be due to the inhomogeneity of the near subsurface materials and other interferences, and detection of this irregular wave-front by one geophone will rise uncertainty representing the mean of the wave-front. Because of this uncertainty the reflection arrival times on the record may become unreadable. To overcome to this difficulty it was suggested to use more than one geophone, so the arrival time shown by a trace approaches reasonably closely the arrival time of the ideal "true" reflection.

In the rest of this study, we will investigate one and two-dimensional geophone arrays which will be called "in-line" and "areal" arrays respectively. Shot generated noise, which is the greatest concern of a geophysicist, may be cancelled by the use of in-line arrays but the inherent property of in-line arrays is the total acceptance of coherent noise in the direction perpendicular to the array.

Shot generated noise contains of coherent waves confined to neighborhoods of boundaries and waves arriving from scattering centers. Scattered waves may be largely disturbances from secondary sources set up by the impinging of the initial near-surface waves upon randomly located near-surface inhomogeneities. In such situations it is important to establish which noise is dominant. In those cases in which both types of waves are sufficiently damaging, it may become necessary to construct two-dimensional arrays having specified responses for particular directions of arrival. By use of properly designed two-dimensional geophone arrays, it is possible to reject such unwanted energy.

COMPUTING RESPONSE OF ARRAYS

A geophone array is a filter system and, therefore, it has an impulse response. Consider an elastic wave travelling along the surface with an apparent velocity V , and as the wave-front hits the geophone, the output of the geophone will be an impulse since the geophones are not distributed continuously in space. This implies, the impulse response of a particular geophone in the space domain may be written as $\delta(x)$ (Hadsell, 1968). The output $s(t,x)$ of a geophone array is related to the ground motion $f(t,x)$ through a convolution

$$s(t,x) = f(t,x) ** a(t,x)$$

where, $a(t,x) \cong b(x)h(t)$. Neglecting the plant-geophone-amplifier-filter characteristics, $h(t)$, the output may be written as $s(t,x) = b(x) * f(t,x)$, where $b(x)$ is the spatial impulse response of the geophone array.

Inline Arrays

A five-equally spaced and weighed geophone array is shown in Figure 3. The parameters which will define an inline array are; number of geophones, N . geophone spacing, Δx , and length of the array, $L = (N-1)\Delta x$.

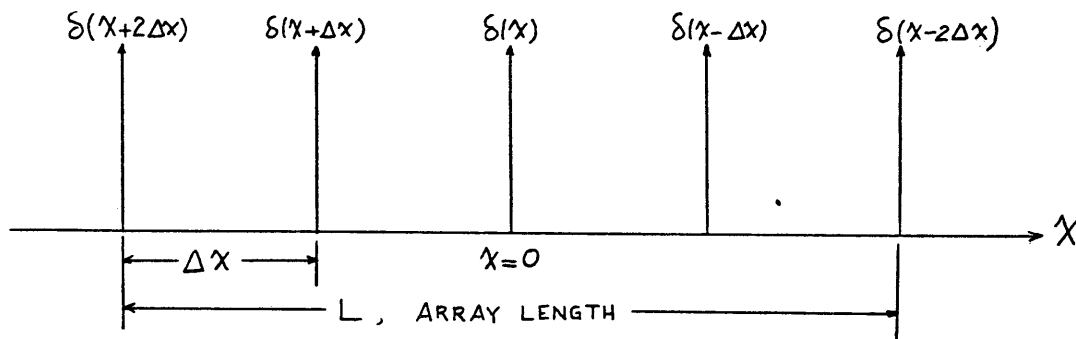


Figure 3. Five-geophone inline array

The spatial impulse response, $b(x)$, of the array shown in Figure 3 is written as

$$b(x) = \delta(x-2\Delta x) + \delta(x-\Delta x) + \delta(x) + \delta(x+\Delta x) + \delta(x+2\Delta x) \quad (4)$$

The steady-state response of a linear system is the response of the system to a sine or cosine input. The steady-state response of the geophone array is obtained by Fourier transforming the impulse response of the array. Since geophone array may be assumed to be consist of a series of dirac impulses, transformation will be achieved as transforming the space-delayed impulses. The spatial frequency represent-

ation of equation (4) is

$$\begin{aligned}
 B(k) &= e^{2\pi j k 2\Delta x} + e^{2\pi j k \Delta x} + 1 + e^{-2\pi j k \Delta x} + e^{-2\pi j k 2\Delta x} = \\
 &= 1 + 2 \left(\cos 2\pi k \Delta x + \cos 2\pi k 2\Delta x \right) \quad (5)
 \end{aligned}$$

In general, the wave-number response of a geophone array which has $N = 2n + 1$ equally spaced geophones weighed with weight coefficients a_i and symmetrically disposed about the array center, will be given by equation (6).

$$B(k) = a_0 + 2 \sum_{i=1}^n a_i \cos 2\pi k i \Delta x \quad (6)$$

Now we will find the response of an infinite number of geophones arrayed over a length L , which is equivalent, one continuous geophone whose length is L . The distribution

$$b_s(x) \triangleq \sum_{i=-n}^n b(i\Delta x) \delta(x - i\Delta x) \quad (7)$$

helps us to represent the sampling in space-domain. This generalized function may also be written

$$b_s(x) = b(x) b_{n,\Delta x}(x) \quad (8)$$

where,

$$b_{n,\Delta x}(x) \triangleq \sum_{i=-n}^n \delta(x - i\Delta x) \quad (9)$$

The spatial frequency representation of equation (9) is given by (Hadsell, 1968)

$$B_{n,\Delta x}(k) = \frac{\sin(2n+1)\pi k \Delta x}{\sin \pi k \Delta x} \quad (10)$$

where $N = 2n+1$ is the number of geophones and $\Delta x = L/(N-1)$ the geophone spacing, substituting these definitions into equation (10) we will have

$$B_{N,\Delta x}(k) = \frac{\sin \frac{N}{N-1} \pi k L}{N \sin \frac{1}{N-1} \pi k L} \quad (11)$$

Letting N approach to infinity and L being fixed, the array of geophones becomes a continuous detector length L ,

$$\lim_{N \rightarrow \infty} B_{N,\Delta x}(k) = \frac{\sin \pi L k}{\pi L k} \triangleq B_{\infty} \quad (12)$$

Using $\text{sinc } X \triangleq (\sin \pi X)/\pi X$ we may write equation (12) as $B_{\infty} = \text{sinc } Lk$. We conclude that the amplitudes of a uniformly weighed continuous geophone array will follow a sinc curve such as that will be plotted in Figure 4.

Areal Arrays

As mentioned earlier in this thesis, in order to cancel the noise waves arriving at the surface spread at large angle of incidence and from arbitrary azimuths, a two-dimensional

geophone array is customarily used. Given the wave-front

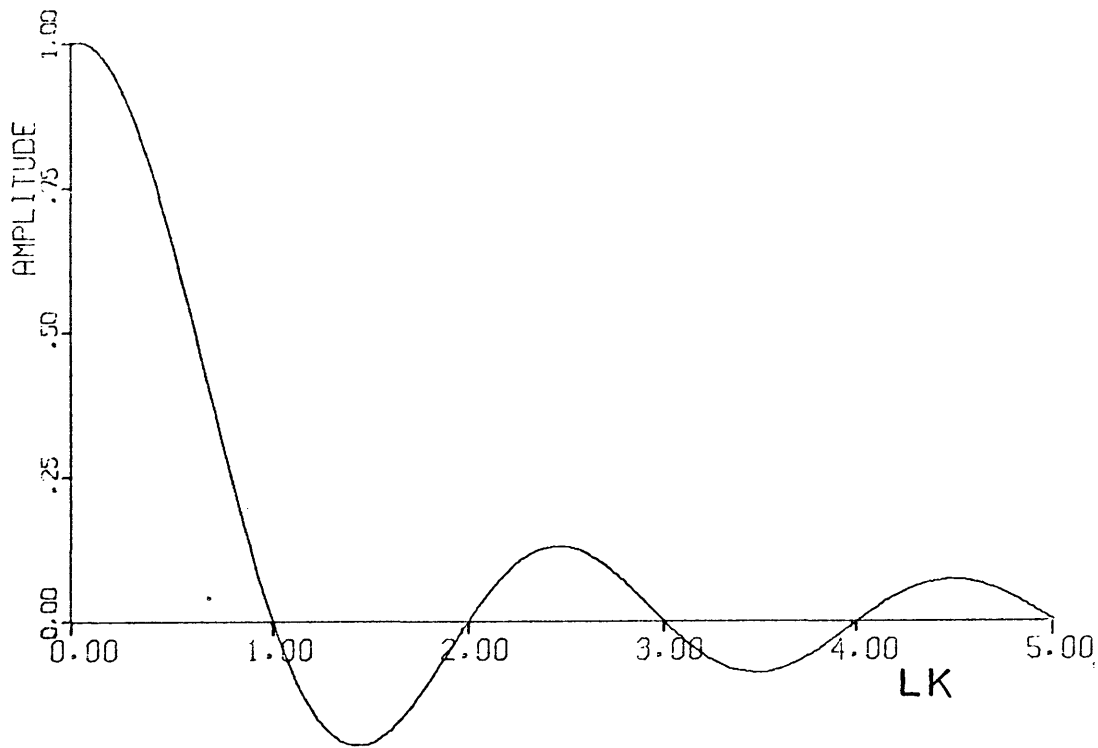


Figure 4. Amplitudes of an equally weighed continuous line of geophones

shape of the incident wave, the response of a two-dimensional geophone array may be obtained by reducing the areal array to an inline array by projecting geophone positions along horizontal traces of wave-fronts. Figure 5 shows a simple nine-geophone two-dimensional array and three different directions of interest. Waves A and B see a three-geophone spread each weighed by three, to wave C, the array is effectively a five-geophone spread and weighed differently. Figure 5 also

shows the impulse response of the geophone spread with respect

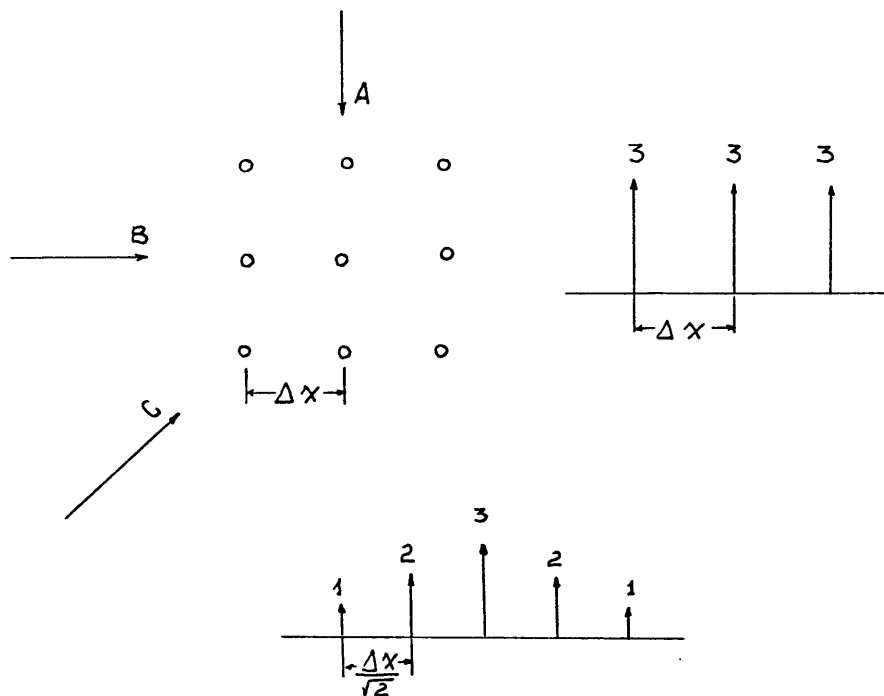


Figure 5. Simple nine-geophone two-dimensional array to the directions of interest.

Two-dimensional Theory of Areal Arrays

Analogous to one dimensional linear systems, it was shown (Hadsell, 1968) that there exists a function $g(x,y) = b(x,y) * f(x,y)$, where $g(x,y)$ and $f(x,y)$ are the output and input of the system respectively, $b(x,y)$ is a distribution characteristic of the geometry of the system. The two-dimensional Fourier transform of $b(x,y)$ which is zero outside of the finite region of the XY-plane is defined by

$$B(k_x, k_y) = \int_{-\infty}^{+\infty} \int_{-\infty}^{+\infty} b(x, y) e^{-2\pi j(k_x x + k_y y)} dx dy \quad (13)$$

where k_x , k_y are the apparent wave-numbers in the X- and Y-directions respectively. This equation describes an analysis of the two-dimensional function $b(x, y)$ into components of the form $\exp[-2\pi j(k_x x + k_y y)]$. As it was said for the inline arrays, the impulse response of a particular geophone in XY-plane may be written in the form of two-dimensional dirac impulse $\delta(x, y)$.

MATHEMATICAL THEORY

Previously many authors worked with the geophone array design problem which will approximate the desired rectangular filter response in the wave-number domain which rejects the wave-numbers greater than the specified value of "K". Figure 6 illustrates signal and noise regions in two-dimensional map view in the wave-number domain. Savit et al (1958) have considered inline geophone arrays with different sensitivity geophones, symmetrically disposed about the array center, and computed weighing coefficients by using the least-square criterion. Holtzman (1963) used minimax polynomial approximation criterion to design the geophone arrays.

The method used here for designing geophone arrays is the approximation of the truncated sinc function in the space domain. Truncation must be taken place at the first zero crossing of the sinc function. This truncation will be achieved by multiplying sinc function with the rectangular window function in the space domain. We will define the

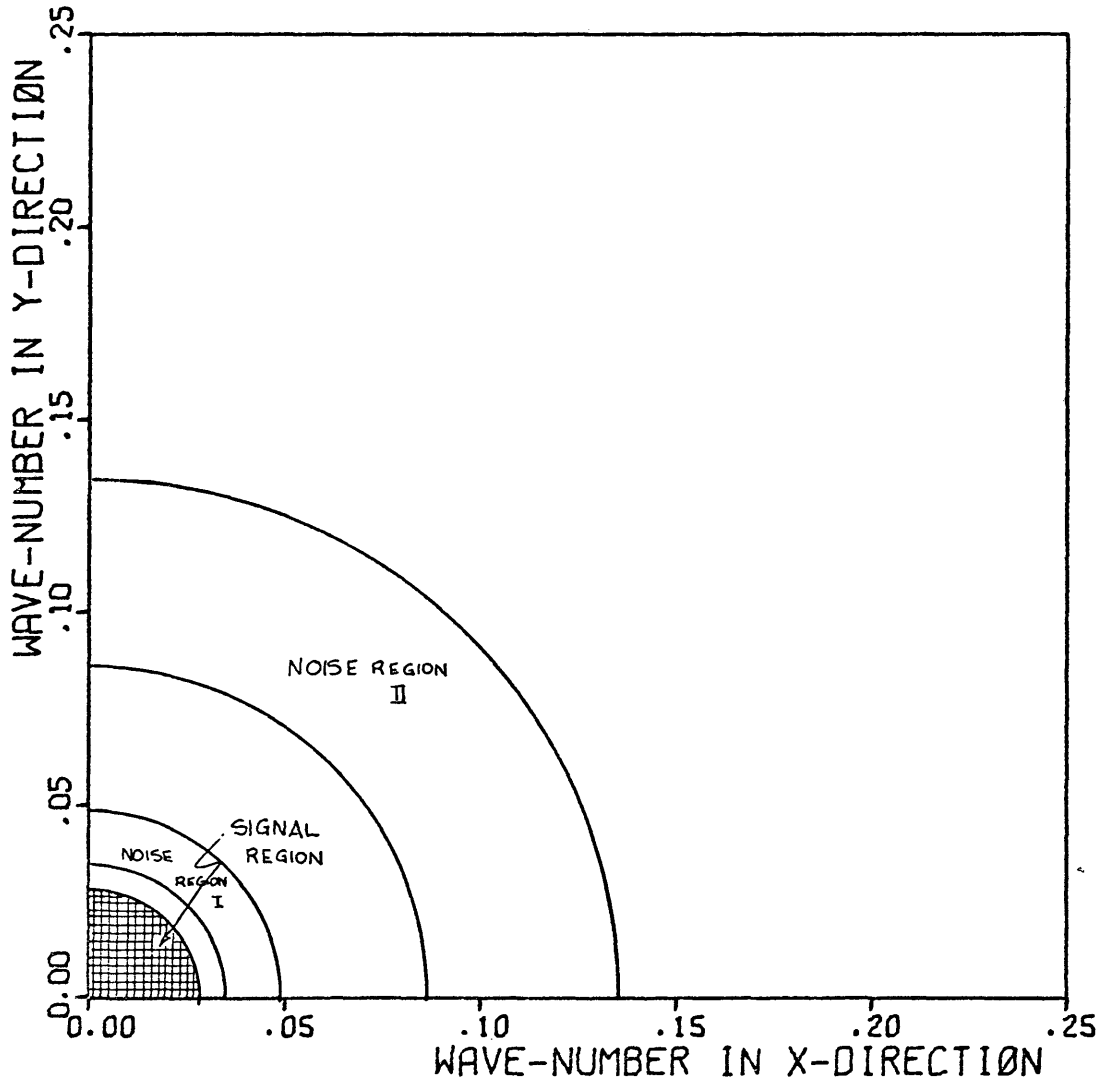


Figure 6. Signal and noise regions

ideal low-pass filter as the filter whose amplitude is constant for $|K| < K_c$ and zero for $|K| > K_c$.

$$A(K) = \begin{cases} A_0 & \text{for } |K| < K_c \\ 0 & \text{for } |K| > K_c \end{cases} = A_0 P_{K_c}(K) \quad (14)$$

Its system function is given by equation (15).

$$H(K) = A_0 P_{K_c}(K) e^{-j2\pi KX} \quad (15)$$

We also want this ideal low-pass filter to be zero phase-shift to preserve the signal characteristics. Figure 7 illustrates this kind of filter.

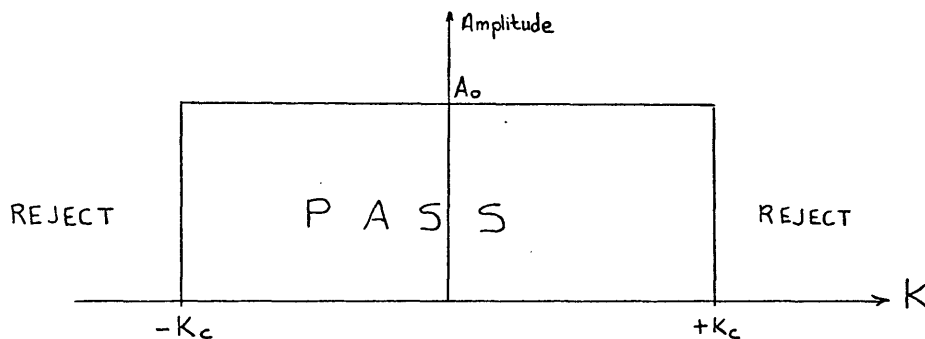


Figure 7. Ideal low-pass filter

This filter response is the rectangular filter response, what we have called from the very beginning. Now, consider a continuous detector of length $L = 1/K_c$, uniformly sensitive over its length. This is shown in Figure 8. Equation (16) is the mathematical expression of Figure 8.

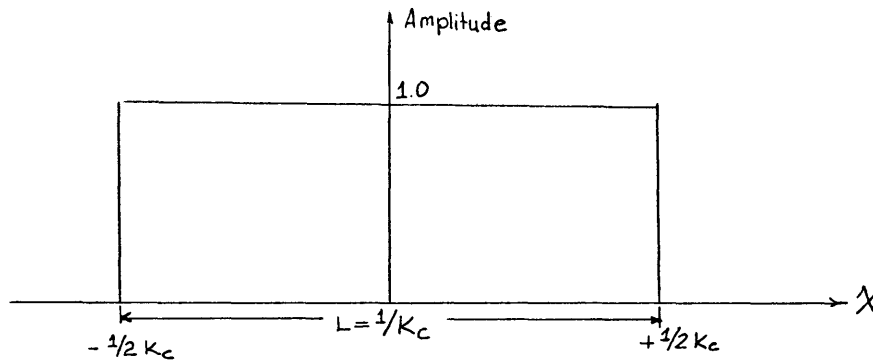


Figure 8. Continuous line of geophones over length L

$$b(x) = p_{\frac{1}{2}K_C}(x) \quad (16)$$

Fourier transforming equation (16), we have (see Figure 4),

$$\begin{aligned} B(K) &= \int_{-\infty}^{+\infty} p_{\frac{1}{2}K_C}(x) e^{-2\pi j K x} dx = \int_{-\frac{1}{2}K_C}^{+\frac{1}{2}K_C} e^{-2\pi j K x} dx = \\ &= \frac{\sin \pi K/K_C}{\pi K} \end{aligned} \quad (17)$$

Multiplying and dividing equation (17) by K_C ,

$$B(K) = \frac{1}{K_C} \frac{\sin \pi K/K_C}{\pi K/K_C} = \frac{1}{K_C} \text{sinc}(K/K_C) \quad (18)$$

The inverse Fourier transform of equation (15) gives

$$a(x) = 2K_C \text{Sinc } 2K_C x \quad (19)$$

Truncation of $a(x)$ with the window function of $b(x)$ gives

$$a(x) b(x) = p_{\frac{1}{2}K_c}(x) 2K_c \text{Sinc } 2K_c x \quad (20)$$

Equation (20) is illustrated in Figure 9. From the properties of Fourier transformation we know that multiplication in space domain corresponds convolution in spatial frequency domain, therefore, we may write equation (21).

$$a(x) b(x) \longleftrightarrow \frac{1}{2\pi} A(K) * B(K) \quad (21)$$

Therefore, we were able to write the approximated rectangular

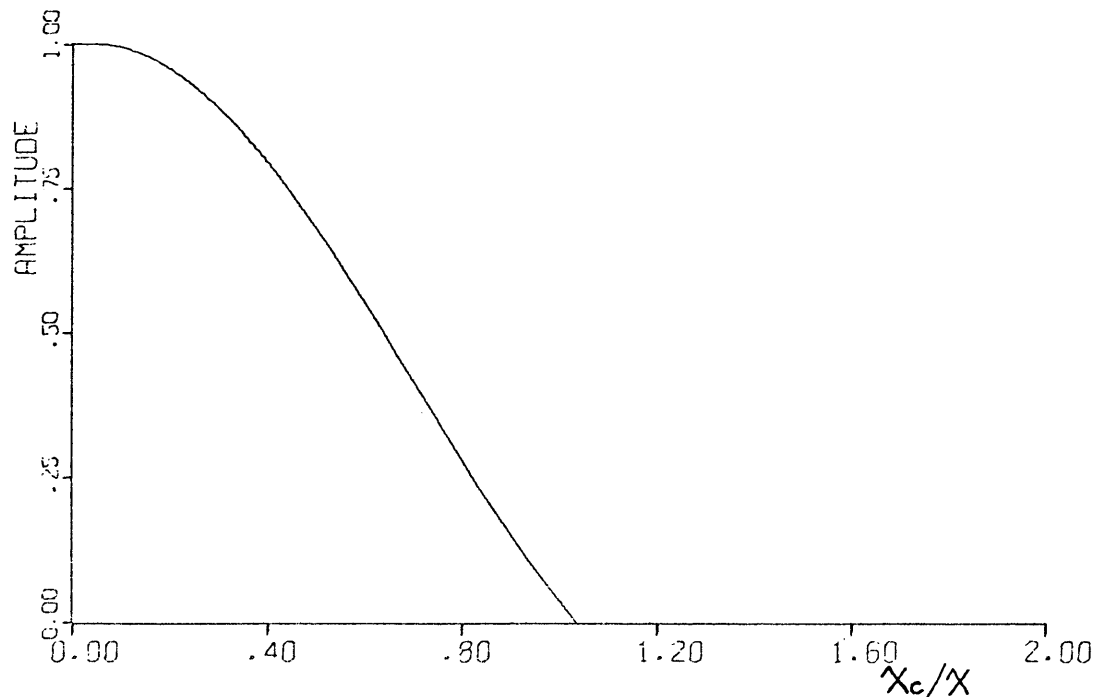


Figure 9. Truncated Sinc function

response in the spatial frequency domain as

$$\frac{1}{K_c} \text{Sinc} (K/K_c) * P_{K_c} (K). \quad (22)$$

To see how well this zero-phase filter does approximate the specified response, we simply find the Fourier transform of the sampled truncated spatial impulse response (Figure 9) represented by $a_{-N}, a_{-N-1}, \dots, a_{-1}, a_0, a_1, \dots, a_{N-1}, a_N$ which is

$$\begin{aligned} B_{ApX}(K) &= \sum_{n=-N}^N \alpha_n e^{-2\pi j K_n \Delta x} = \\ &= a_0 + 2 \sum_{n=1}^N \alpha_n \cos 2\pi K_n \Delta x, \quad \text{since } \alpha_{-n} = \alpha_n. \end{aligned} \quad (23)$$

Now, $B_{ApX}(K)$ should approximate the specified low-pass characteristics of Figure 7. $B_{ApX}(K)$ is given in Figure 10.

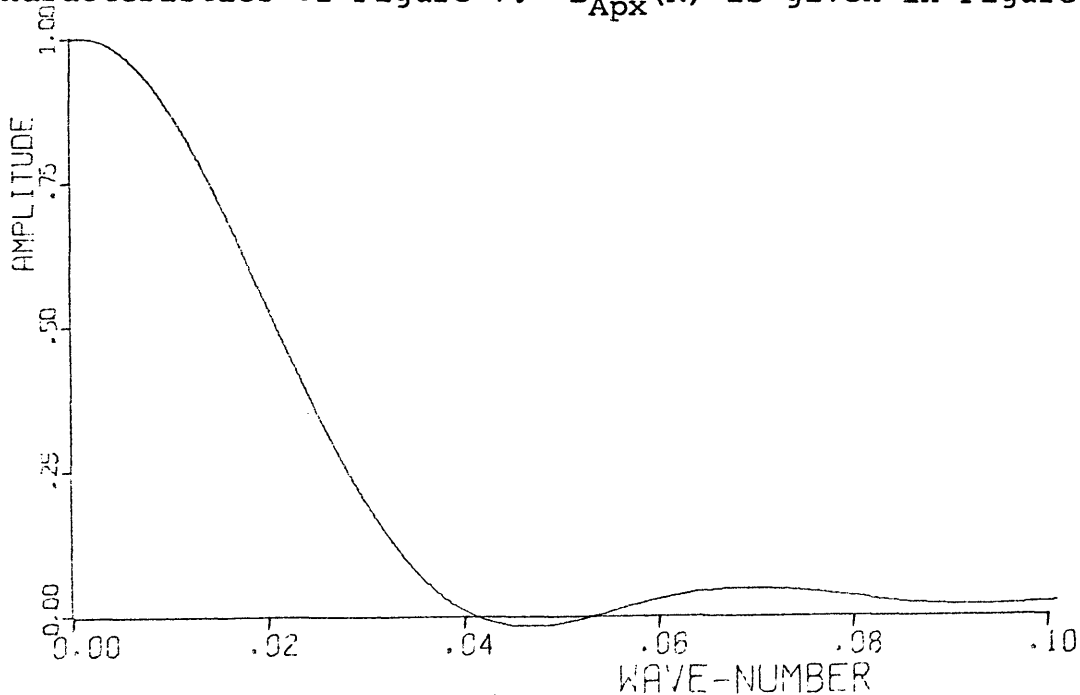


Figure 10. Fourier transform of truncated Sinc function

Doubling the sample interval will halve the sample frequency, therefore, we obtain similar performance with fewer samples but we pay for it by reducing the Nyquist wave-number to $K_N = 1/2 (2\Delta x)$. From equation (10), we may also see that changing Δx while keeping L constant will change a normalized $B(K)$ principally in the rejection band.

The choice of this approximation may be justified as follows: (1) We want a rectangular response in the wave-number domain. (2) The inverse Fourier transform of this response gives a Sinc function in space domain. (3) If we were able to place geophones continuously on a line, the amplitudes of this spread should follow a Sinc function which gives a rectangular response as a Fourier transform. (4) If we multiply these two "ideal" forms in space domain we will end up with the truncated Sinc function.

The Fourier transform of the truncated Sinc should approximate the desired rectangular wave-number response.

Truncation of $(\text{Sin}\pi x)/\pi x$ was introduced by Gangi and Disher (1968). Disher (1968, p. 92) said, "This should give a sharply cut-off, low-pass filter. The truncation will prevent: 1. The amplitude response of having an infinite slope in frequency at the cut-off frequency, and

2. Infinite attenuation above the cut-off frequency". By truncation the Sinc function in the space-domain at the first zero we achieved another important property in that the geophones will be connected with the same polarity.

COMPUTING TWO-DIMENSIONAL RESPONSE OF ARRAYS

We agree that geophone arrays behave as wave-number filters. The amplitude responses of such filters can be obtained by the Fourier transformation of their spatial impulse responses. A fundamental property of Fourier transform is the property that sampling at equal intervals in one domain results periodicity in the other domain. The spatial domain samples at Δx results in a periodic spatial frequency spectrum whose spectral period is $1/\Delta x$. The spatial frequency $K_N = 1/2\Delta x$ is called the folding frequency because the spectral content in frequency range above K_N is folded back into the primary-spectral range below K_N . To avoid spatial frequency aliasing, the distance domain sampling interval (geophone spacing) must be chosen such that K_N is greater than the upper spatial frequency band limit K_C of the data. The region of the space bounded by the two axes, the vertical line at K_{Nx} and the horizontal line at K_{Ny} is called the primary region. Now consider an

array $b(x,y)$ which is real, this implies in the spectral domain (Papoulis, 1968), $B(K_x, K_y) = B(-K_x, -K_y) = B^*(K_x, K_y)$ and if $b(x,y) = b(-x,y) = b(x,-y) = b(-x,-y)$, then $B(K_x, K_y)$ is real and $B(K_x, K_y) = B(K_x, -K_y) = B(-K_x, K_y) = B(-K_x, -K_y)$. Therefore, for the arrays which have the above spatial and spectral properties, the two-dimensional amplitude spectrum throughout the space is specified by the amplitude spectrum in primary region.

In computing the two-dimensional geophone arrays, parameters are selected to be general enough to be used with any array of the same configuration but not necessarily of the same physical dimensions. That is, the two-dimensional array responses are described in terms of dimensionless products, $K_x \Delta x$ and $K_y \Delta y$, rather than in terms of length in feet and spatial frequency (wave-number) in cycles per foot. Therefore, the response maps are presented as, the contours of the amplitude values, and axes being the product of the geophone spacing and the apparent wave-number in two perpendicular directions. The range of $K_x \Delta x$ and $K_y \Delta y$ runs from zero to one-half.

The amplitude spectrum of the geophone arrays were computed using the straightforward two-dimensional Fourier

transform formula and CSM's PDP-10 time-sharing computer system. Equation (14) can be written as

$$B_{K_y, K_x} = \sum_{m=0}^{M-1} \sum_{n=0}^{N-1} D(m,n) e^{-2\pi j (K_x n \Delta x + K_y m \Delta y)} \quad (24)$$

where $D(m,n)$ is the array weights. As an example consider the following diagram (Figure 11) of a nine-geophone square array. The array has been placed in the first quadrant. Input to the program would be the coordinates of each geophone in terms of m , n , and amplitude of each geophone, usually equal to 1.0.

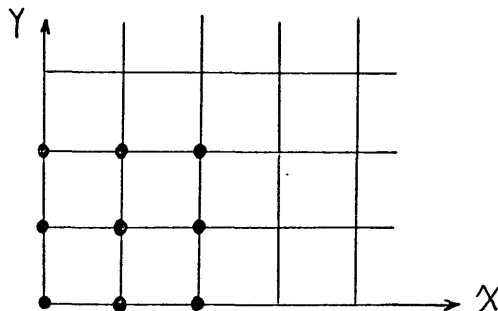


Figure 11. Nine-geophone array in XY-plane

The sequence of operations can be visualized clearly with the help of a flowchart, as shown in Figure 12. Figure 12 also illustrates the necessary operations for mapping the two-dimensional array of $B(K_y, K_x)$.

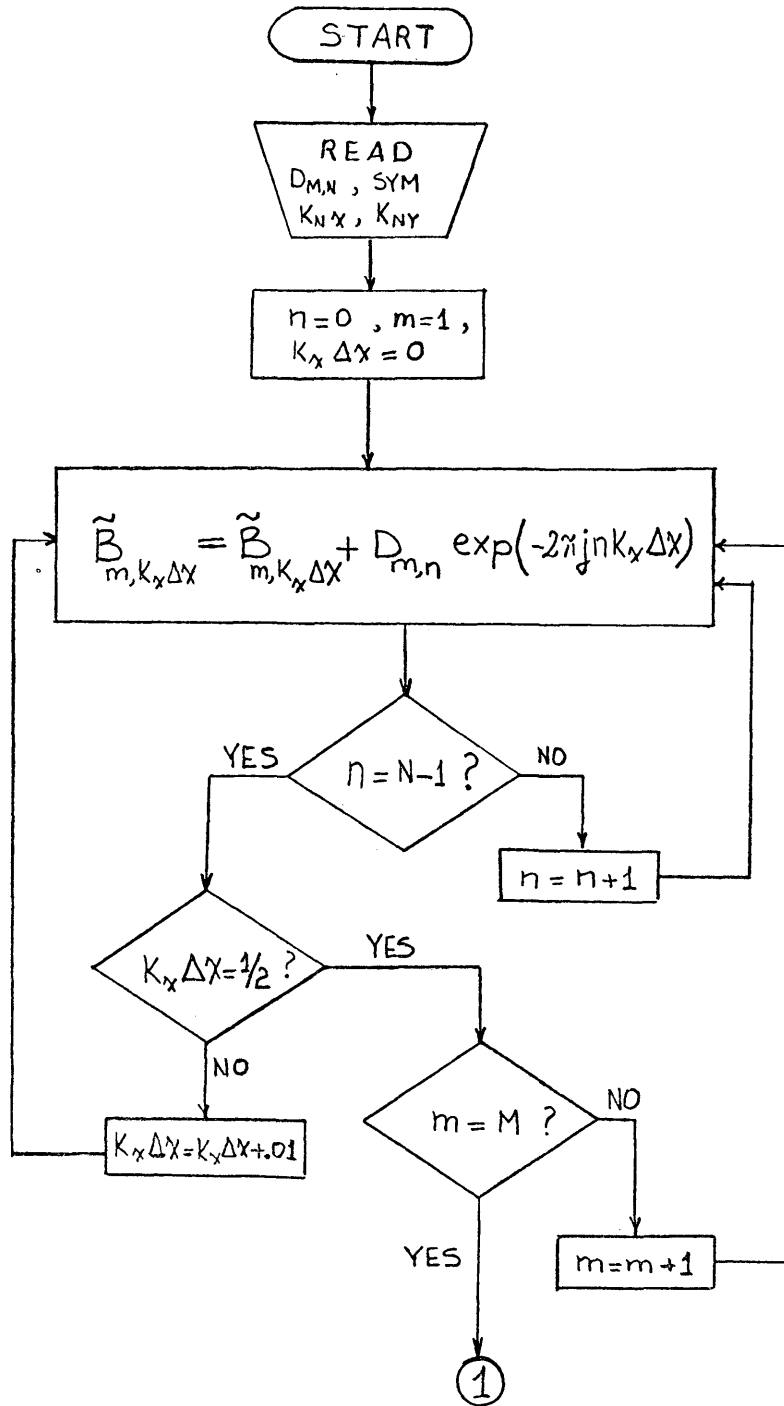
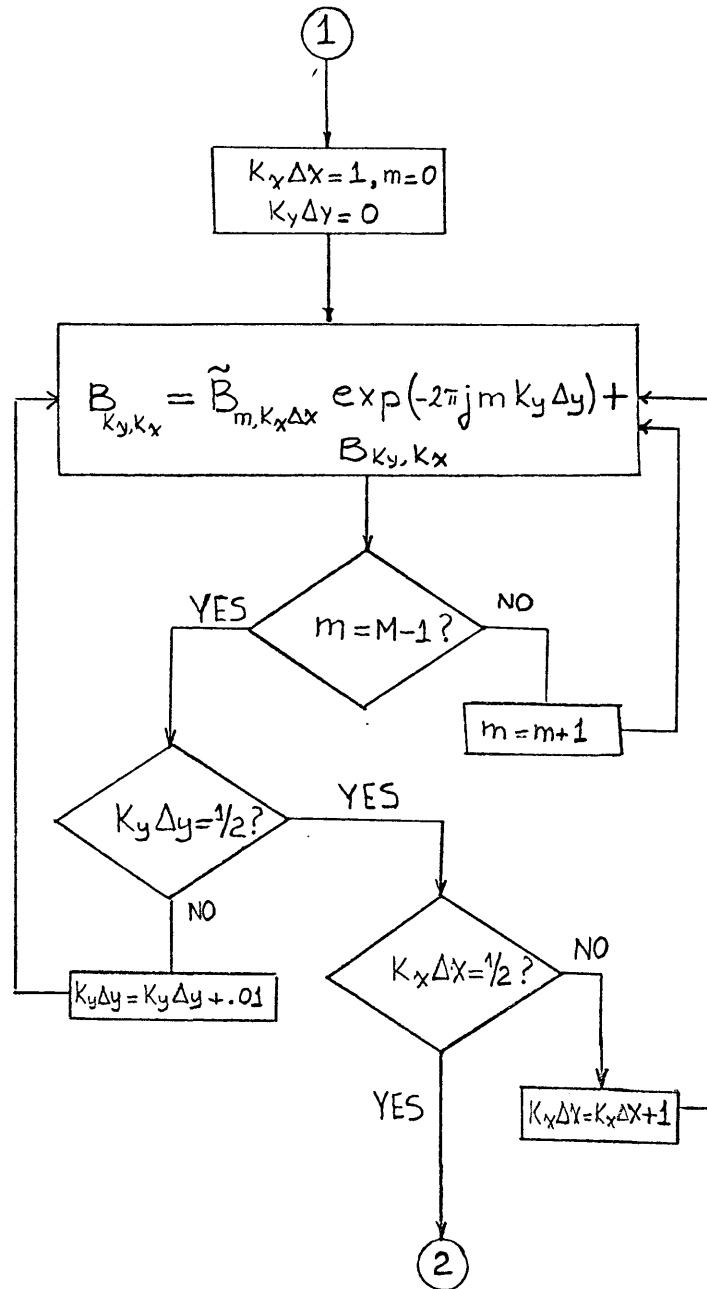
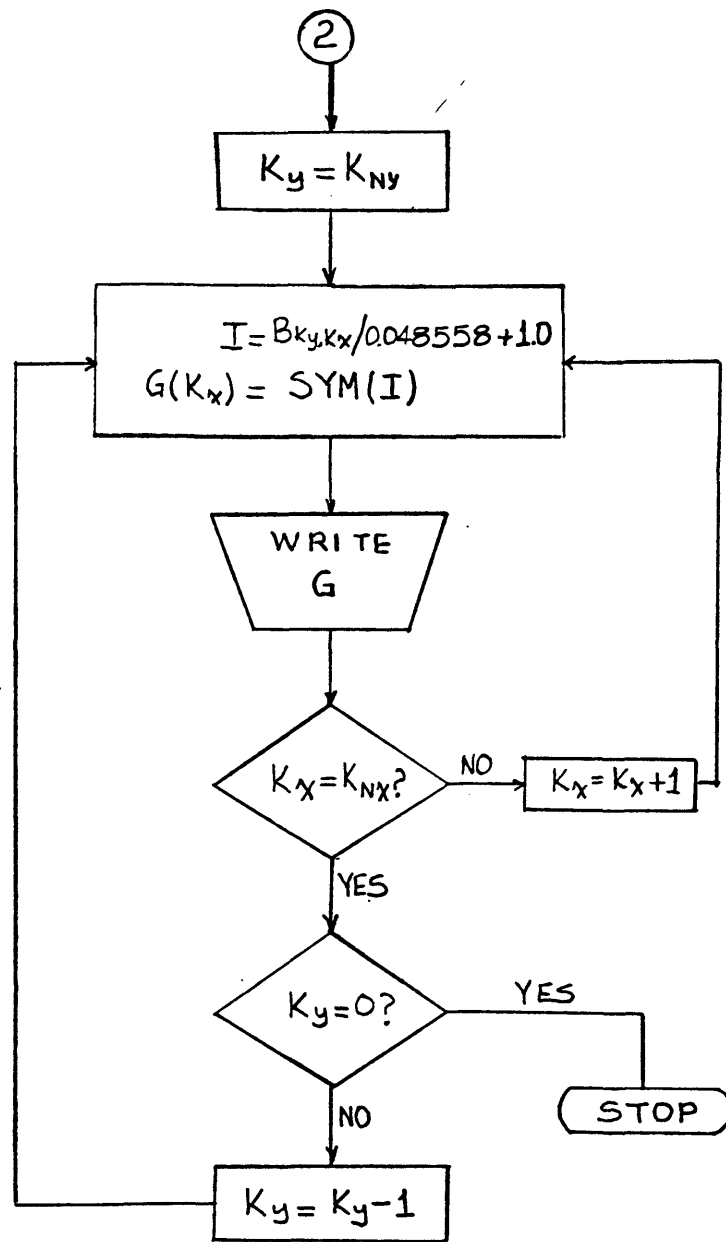


Figure 12. Flowchart of the two-dimensional Fourier transform of a geophone array and mapping of the amplitude response





COMPARISON OF ARRAYS

The amplitude response maps of geophone arrays designed by approximating the truncated Sinc function and of some undesirable arrays will be given in this section.

Array A (Plates 1-3)

If the noise from every direction but along the cable is not much of a problem and a limited number of geophones are available, then the inline arrays are the most economical ones to design and to use. The examination of the response maps shows the acceptance of every wave-number without attenuation for the wave-fronts which are parallel to the inline array. For the energy arriving at the array from other azimuths some wave-number components are attenuated. Narrow wave-number pass-bands require longer arrays. The geophone arrays shown in Plates 1-3 are symmetric with respect to the array center, therefore, the phase response in X-direction is either zero or π . Comparison of the response maps (Plates 1-3) also shows that, amplitude

response of the array shown in Plate 3 is better than the other two. This is due to the good approximation of the truncated Sinc function in the space domain which was shown in Figure 9. The geophysicist must consider areal arrays if the noise and/or the signal is best described in terms of two spatial dimensions.

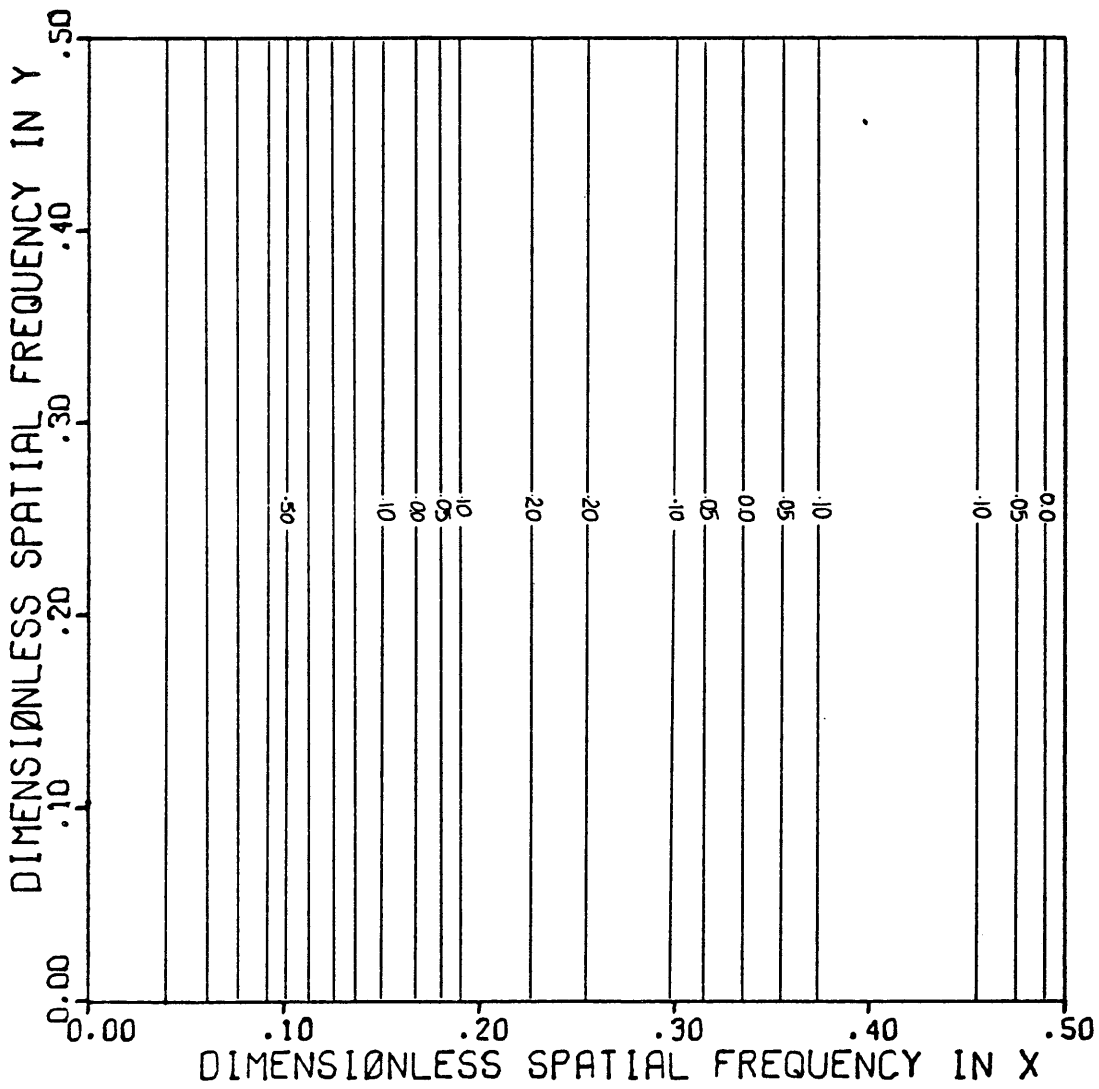
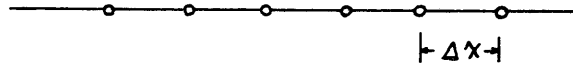


PLATE 1
Uniformly weighed 6-geophone Array A

Square Arrays and Array B (Plates 4-7)

These two shapes of arrays will be discussed together because Array B is actually same as square array but is rotated by an angle $\pi/4$ with respect to the main cable. If we introduce the polar coordinates

$$x=r \cos\theta \quad y=r \sin\theta \quad K_x=\xi \cos\varphi \quad K_y=\xi \sin\varphi$$

then we can write for the square array

$$b(r,\theta) \longleftrightarrow F(\xi,\varphi).$$

If $b(x,y)$ is rotated by an angle $\theta_0 = \pi/4$, then it follows from Papoulis (1968) that its Fourier transform $B(K_x, K_y)$ is also rotated by the same angle, then we may write

$$b(ar, \theta + \theta_0) \longleftrightarrow \frac{1}{a^2} B\left(\frac{\xi}{a}, \varphi + \theta_0\right)$$

Square Arrays (Plates 4, 6)

Examination of amplitude response maps shows that at an angle $\pi/4$ to the main cable, the response well approximates the ideal response, but in the directions of cable and perpendicular to it acceptance of the other disturbances is evident.

Array B (Plates 5, 7)

These arrays give good rejection outside of the pass-band for wave-fronts parallel to or normal to the X-direction.

The acceptance of the unwanted amplitudes is less than 0.10, therefore, we were able to get at least 90% rejection outside of the pass-band. Due to the symmetry of the array at 45 degrees from the X-direction these arrays show less rejection. The alias zones are evident. Increasing the number of geophones used in the array decreases the extent but not the amplitudes of the secondary peaks at 45 degrees, and decreases the extent of the pass-band. By no means could we eliminate the alias zone because of the periodic nature Fourier transforms of uniform fields of spikes.

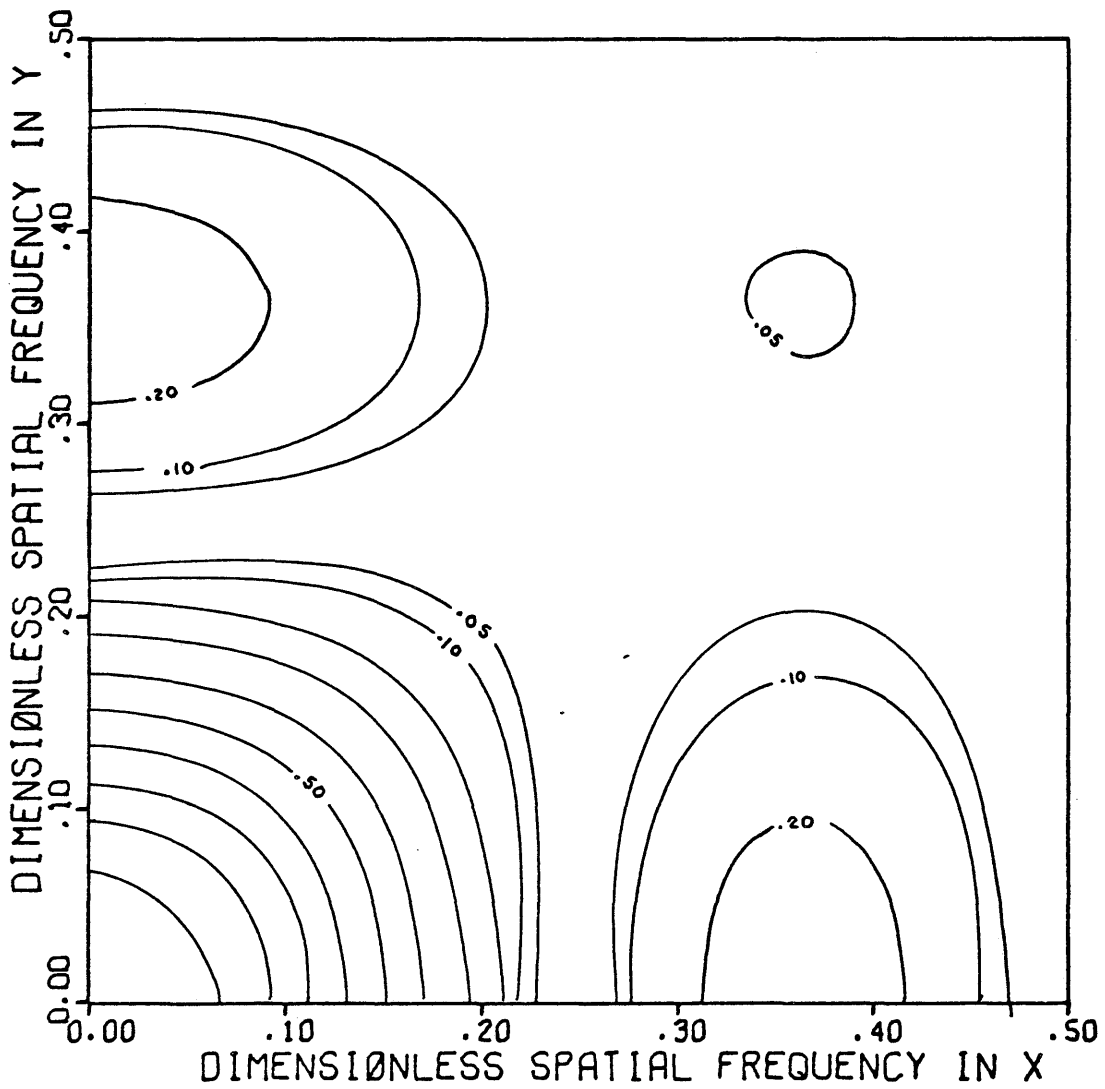
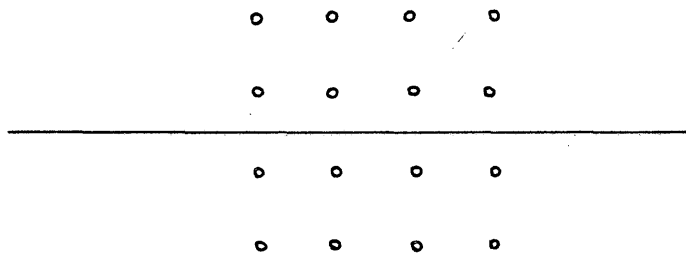


PLATE 4

16-geophone Square Array

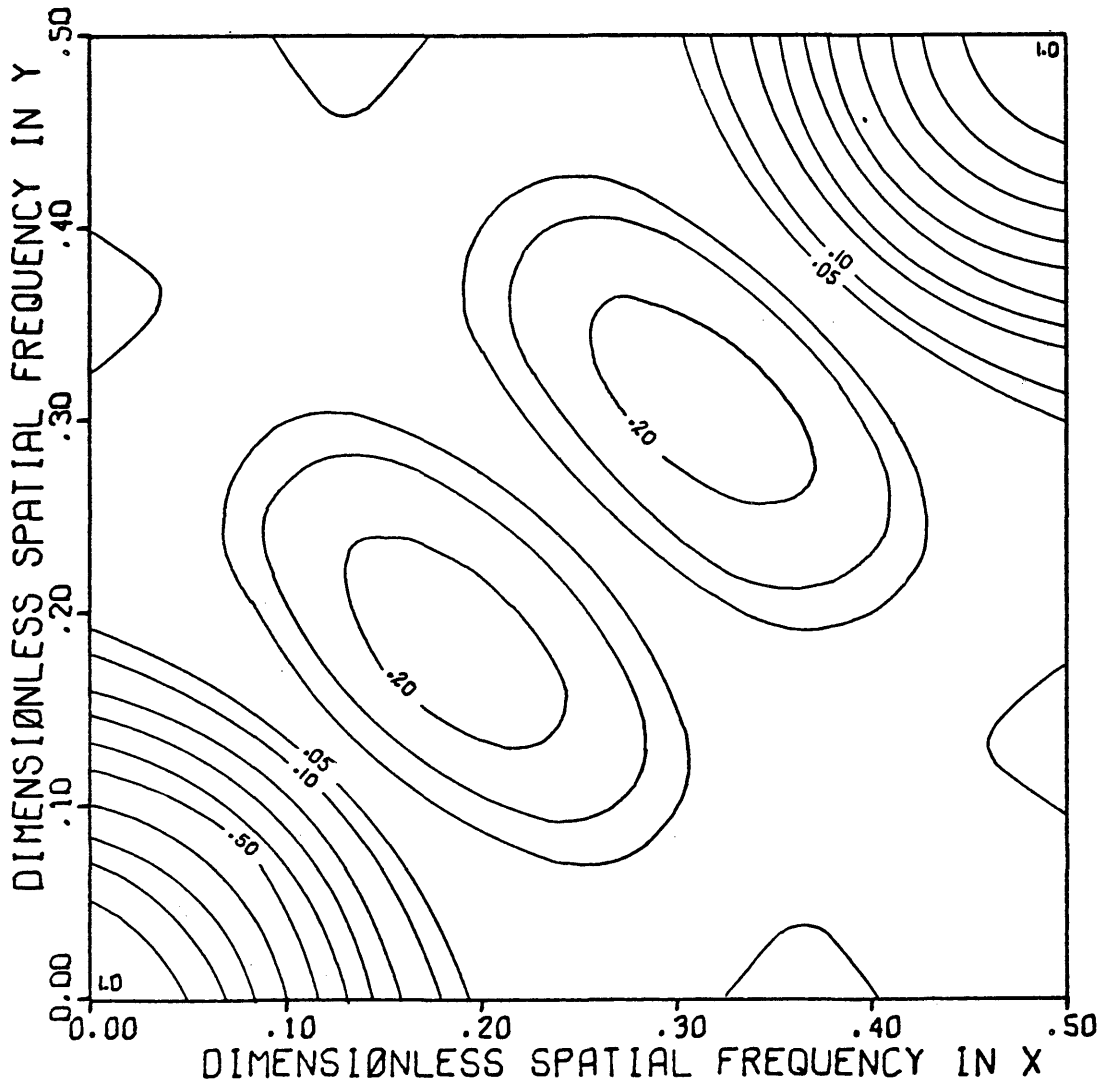
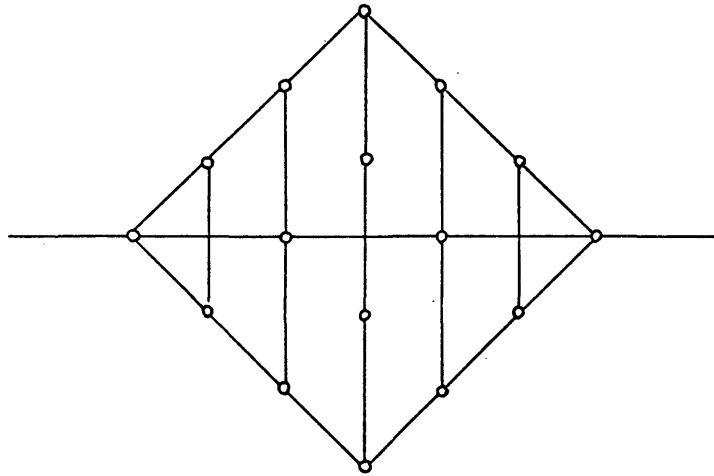


PLATE 5

16-geophone Array B

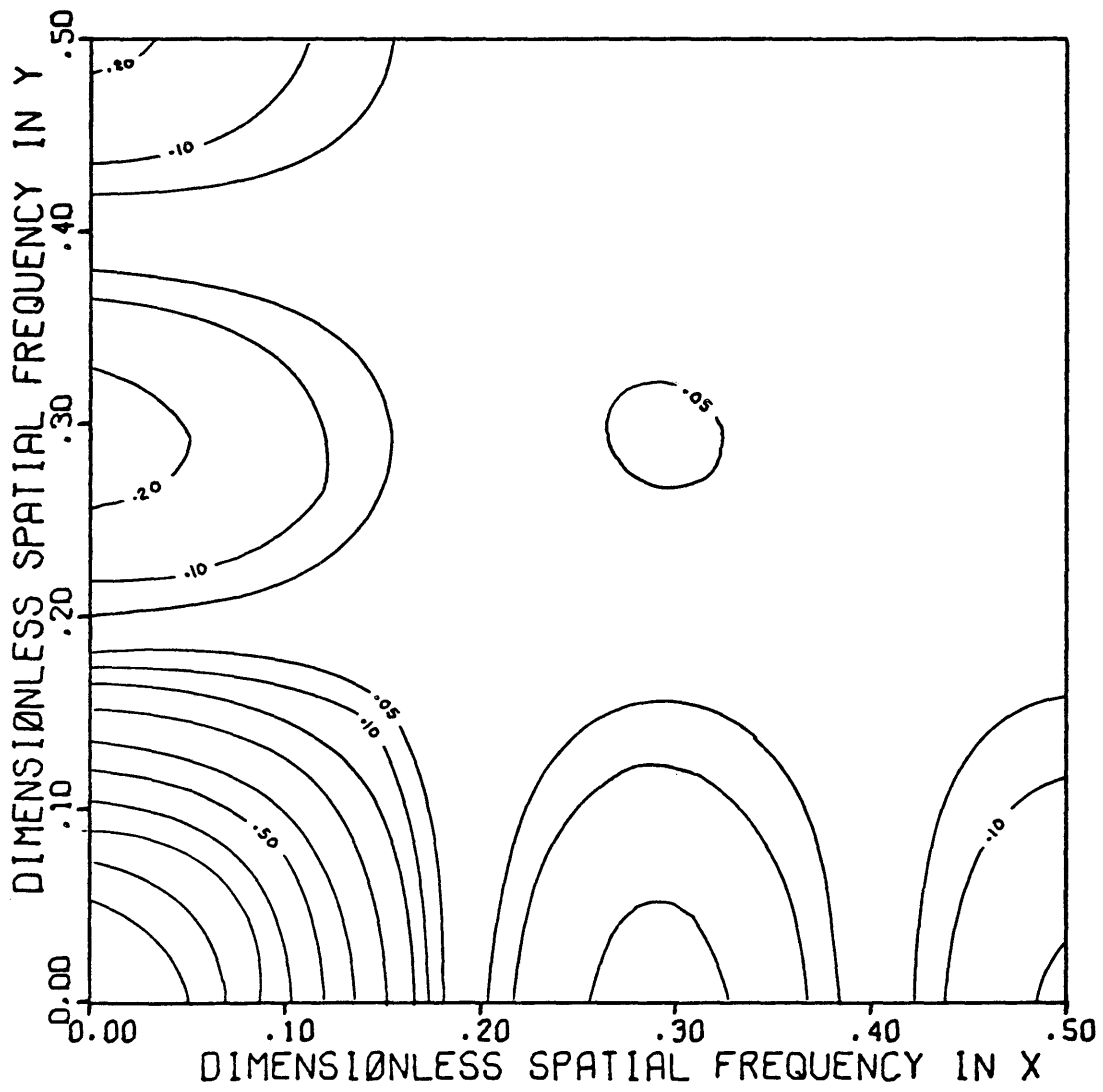
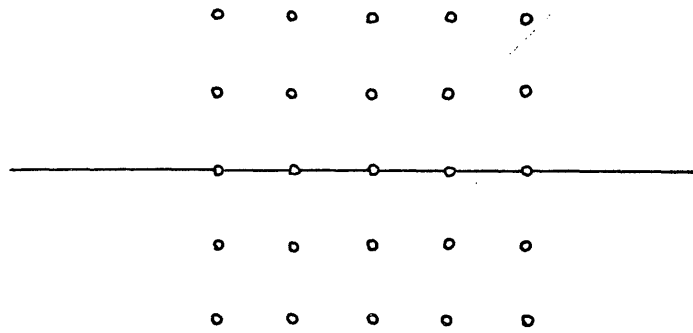


PLATE 6

25-geophone Square Array

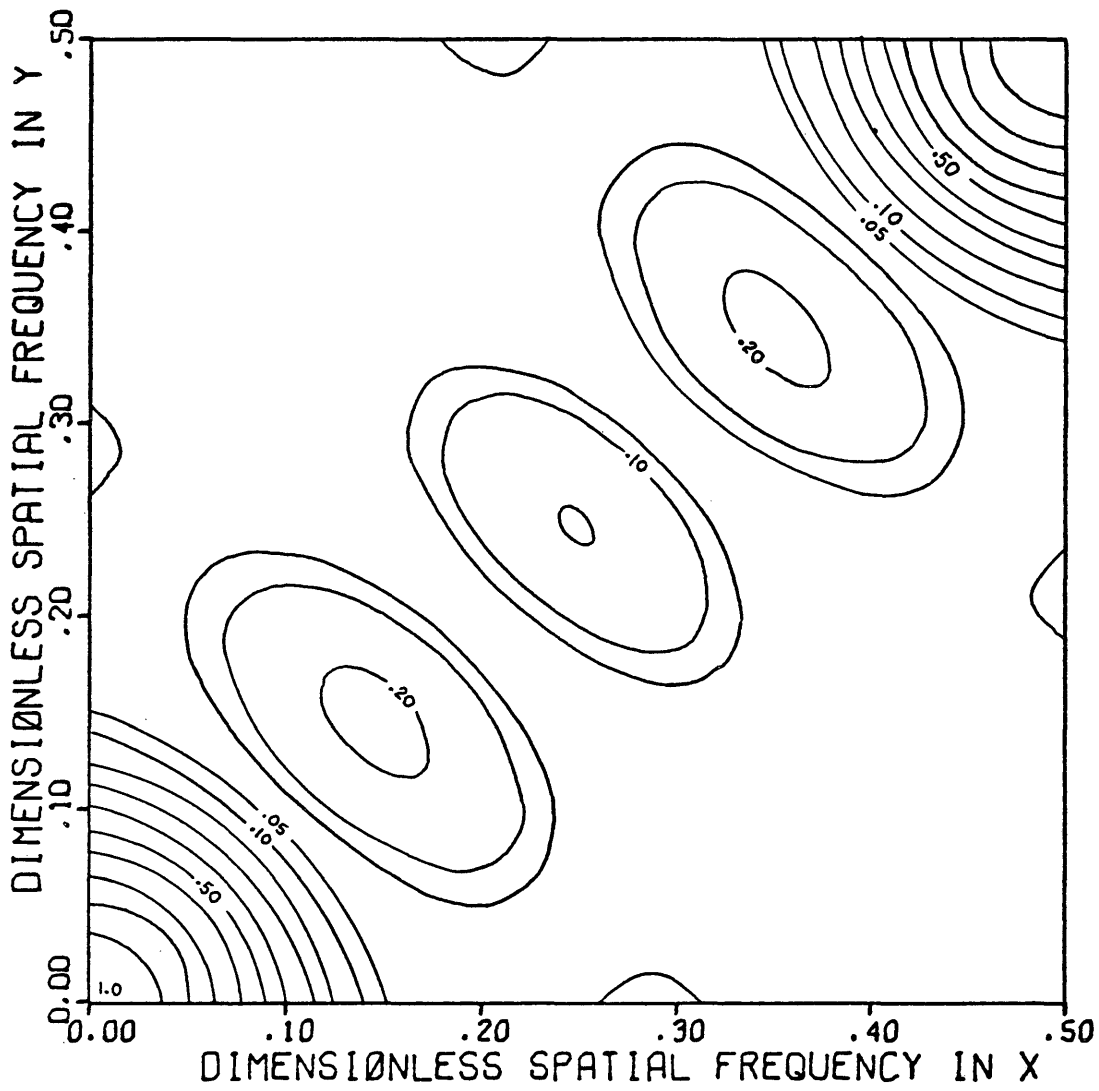
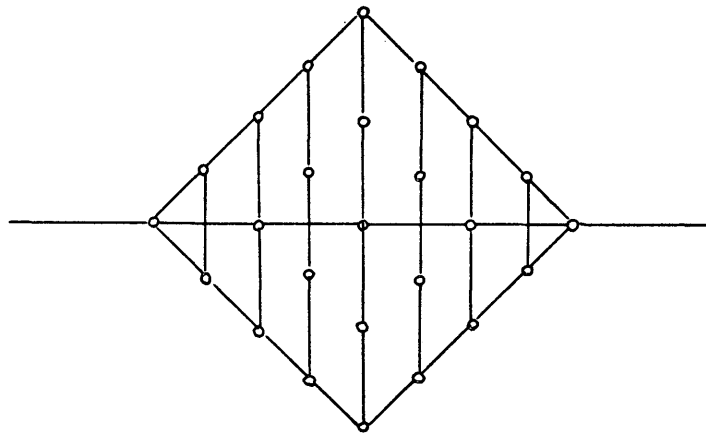


PLATE 7

25-geophone Array B

Array C (Plates 8,9)

The number of geophones used to construct arrays B, arrays C, and the square arrays was taken to be same for ease of comparison. Array C can be easily obtained from the square array by deforming the square array while keeping the geophones with the same ordinate values. The deformation of the square array is illustrated in Figure 13.

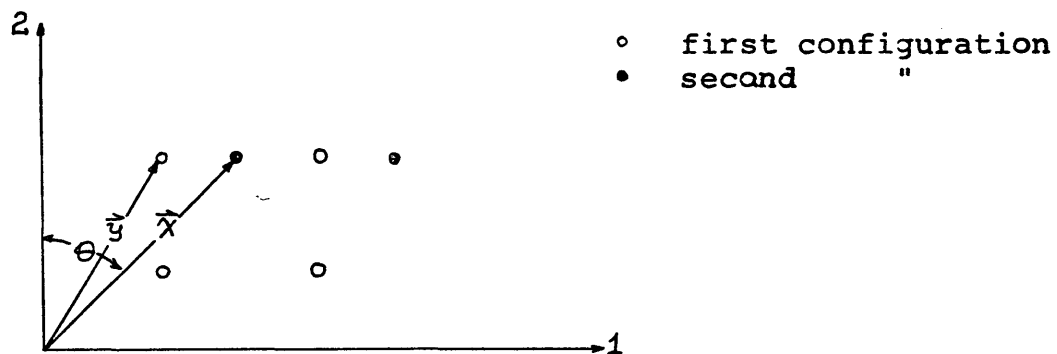


Figure 13. Deformation of four-geophone array

If $b(y^1, y^2) \leftrightarrow B(\psi_1, \psi_2)$,

$$g(y^1, y^2) \triangleq b(y^1, y^2) ** \delta(y^1 - c^1, y^2 - c^2) = b(y^1 - c^1, y^2 - c^2) , \quad (25)$$

and $g(y^1, y^2) \leftrightarrow G(\psi_1, \psi_2)$, then the two-dimensional spectra of $g(y^1, y^2)$ can be computed in terms of the two-dimensional spectra of the unshifted array, $b(y^1, y^2)$, using

$$G(\psi_1, \psi_2) = K B(\psi_n K_1^n, \psi_n K_2^n) \quad (26)$$

In equation (26) K_r^n is the inverse to a system k_r^r in the

sense that $Kr_k^r = \delta_i^n$, where repeated indices imply summation. Here $k_i^r \triangleq \delta_i^r - c_i^r$ where $c^n = c_i^n y^i$.

To prove equation (26), we first write the two-dimensional Fourier transform of $g(y^1, y^2)$ as,

$$G(\Psi_1, \Psi_2) = \iint_{-\infty}^{+\infty} b(y^1 - c^1, y^2 - c^2) \exp[-j \Psi_n y^n] dy^1 dy^2 \quad (27)$$

If we use the change of variables $x^n = k_i^n y^i$ in equation (27), then, we have

$$y^n = K_i^n x^i \quad (28)$$

By substituting equation (28) into equation (27), we obtain

$$G(\Psi_1, \Psi_2) = \iint_{-\infty}^{+\infty} b(x^1, x^2) \exp[-j \Psi_n K_i^n x^i] K dx^1 dx^2 \quad (29)$$

where $K \triangleq |K_i^n|$ is the Jacobian of the coordinate transformation used in the change of the variables of integration. The c_i^r used in this thesis are

$$c_i^r = \begin{bmatrix} 0 & c \\ 0 & 0 \end{bmatrix}, \text{ where } c = \tan \theta.$$

Thus,

$$k_n^i = \begin{bmatrix} 1 & -c \\ 0 & 1 \end{bmatrix}, \quad K_i^n = \begin{bmatrix} 1 & c \\ 0 & 1 \end{bmatrix} \quad (30)$$

It is easily seen from equation (30) that, $K=1$, and using equation (26), we obtain

$$\Psi_n K_i^n = [\Psi_1, \Psi_2] \begin{bmatrix} 1 & c \\ 0 & 1 \end{bmatrix} = \begin{bmatrix} \Psi_1 \\ c\Psi_1 + \Psi_2 \end{bmatrix} \quad (31)$$

Using the above method, equation (31), we can find the amplitude response of any deformed geophone array from the amplitude response of the undeformed geophone array. Figure 14 illustrates how the amplitude response of a deformed geophone array can be calculated by the use of the response map of an undeformed array.

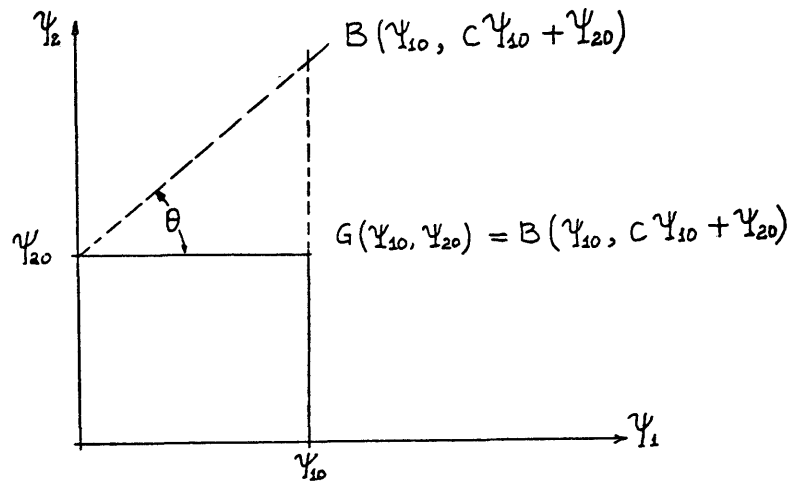


Figure 14. Sketch to find amplitude response of a deformed array

These shapes of arrays also give good rejection characteristics of the unwanted energy wave-numbers for the energy arriving at the array along the main cable from the positive x-direction. For example, note the reduction of the rebound zone at the wave-numbers (0.36 , 0.00). Therefore, this shape of array is more effective than the array B

if the noise energy was from 0 degrees to 65 degrees but poorer if the noise was from 0 degrees to -65 degrees. If the noise analysis shows the energies coming from a direction which is perpendicular to the array, then this pattern shows acceptance of unwanted energy in this particular direction. Again, increasing the number of geophones used in the array will well approximate the desired response in the directions of 0 degree to 45 degrees from the main cable and also increase the rejection angle to 75 degrees (see Plate 9). Therefore, the decision must be made more carefully selecting B or C shape of arrays considering directions of noise arrivals.

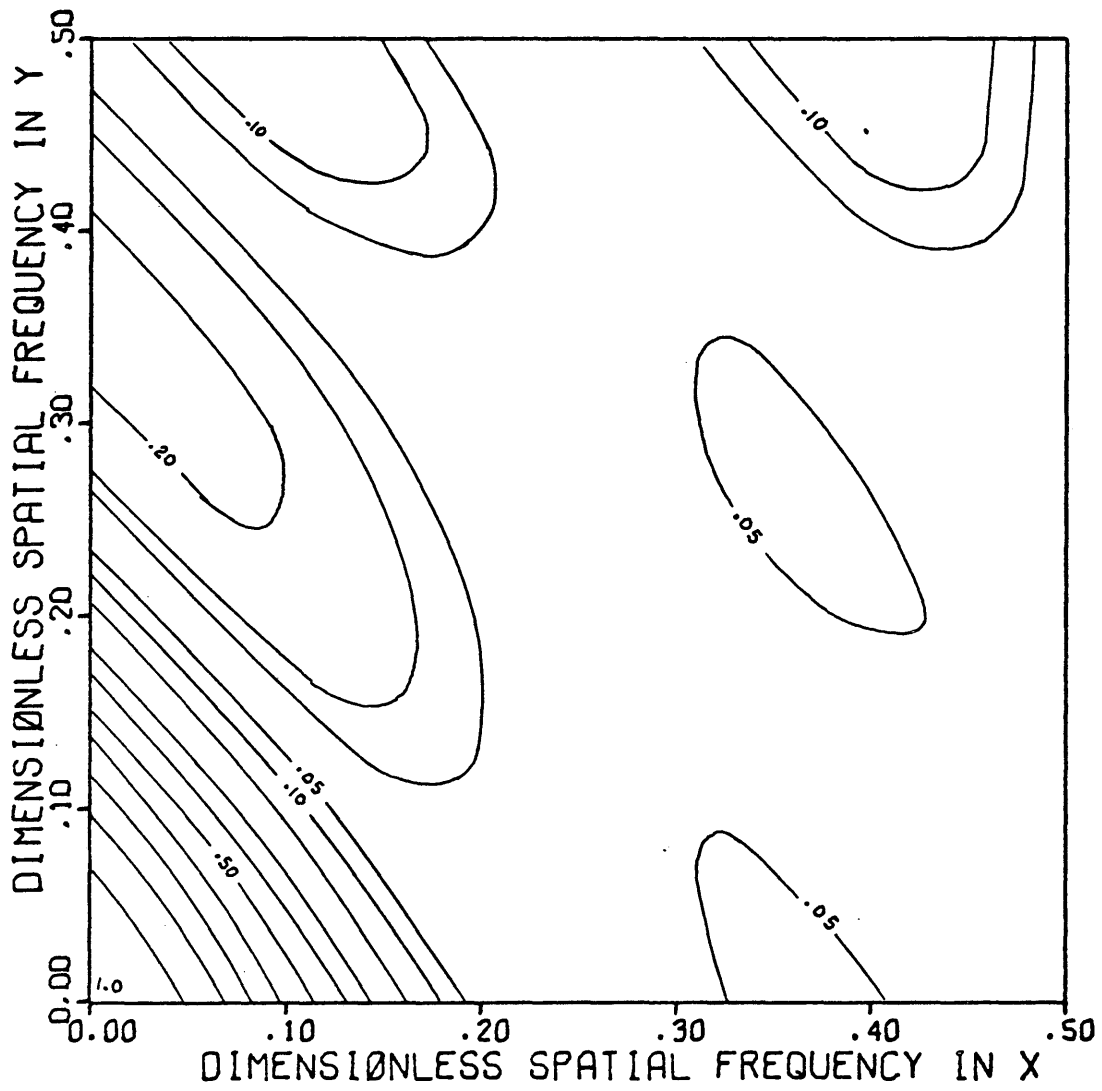
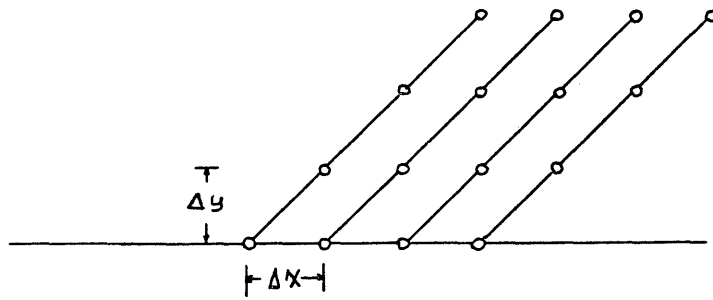


PLATE 8

16-geophone Array C

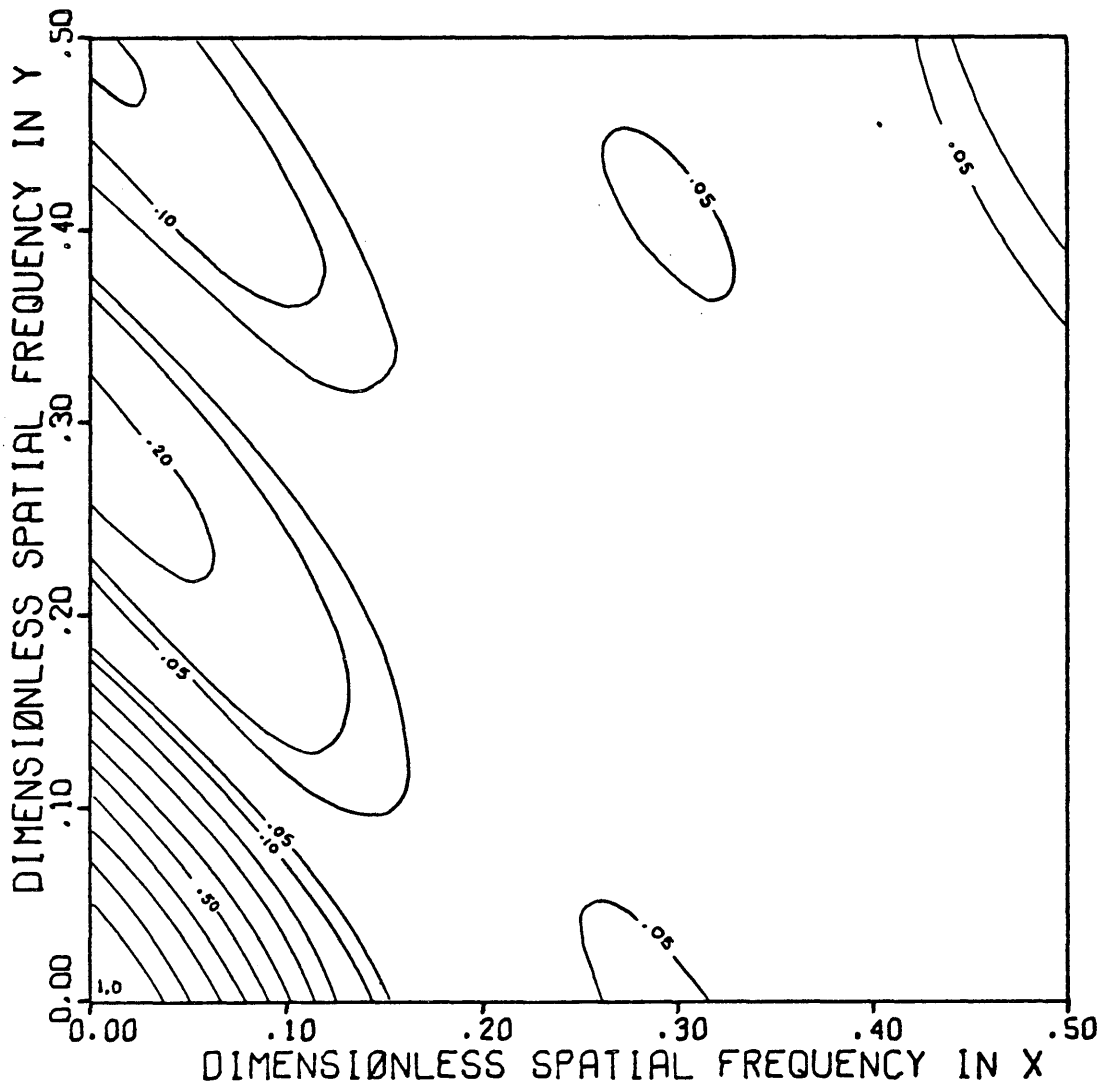
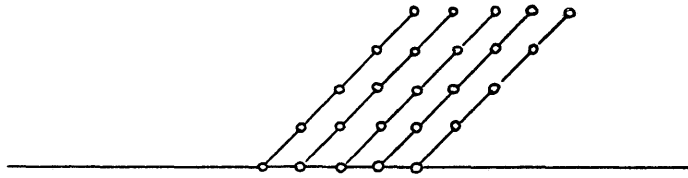


PLATE 9

25-geophone Array C

Array D (Plates 10, 11)

In this shape, the number of geophones used for shape C was doubled. Comparison between sixteen-geophone array C and thirtytwo-geophone array D shows the surprising result that the array C is more effective and more uniform than the later in spite of the number of geophones used in the later is larger than the first one. This shape of array too, gives good rejection from zero wave-number to K_N -dimensionless spatial frequency, in which it approximates the "ideal" response in one direction which is along the main cable.

Rectangular Arrays (Plates 12, 13)

Rectangular shaped arrays too, give undesirable responses for the energies having dimensionless spatial frequencies ranging from 0.09 to 0.5 perpendicular and parallel to main cable.

Star Arrays (Plates 14-16)

The circular arrays, Plate 14, are the most practical ones as far as the lay-out is concerned and they also give sharp cut-offs for the smaller wave-numbers but the characteristics in the rejection areas is poor. Plate 15 illustrates a star array designed using truncated sinc approximation approach and it is easily seen that this pattern is more

uniform and more effective than the array whose response was mapped in Plate 14, even though the number of geophones used to construct the array in Plate 14 is more than that of Plate 15. Plate 16 shows non-uniform star array. Sharpness of the pass-band and almost complete rejection of wave-numbers of inline noise are due to the weighing of the star array by the sinc criterion. Since these types of arrays have circular symmetry, the array responses can also be given as functions of radial and azimuthal wave-numbers instead of K_x and K_y by employing Hankel transforms.

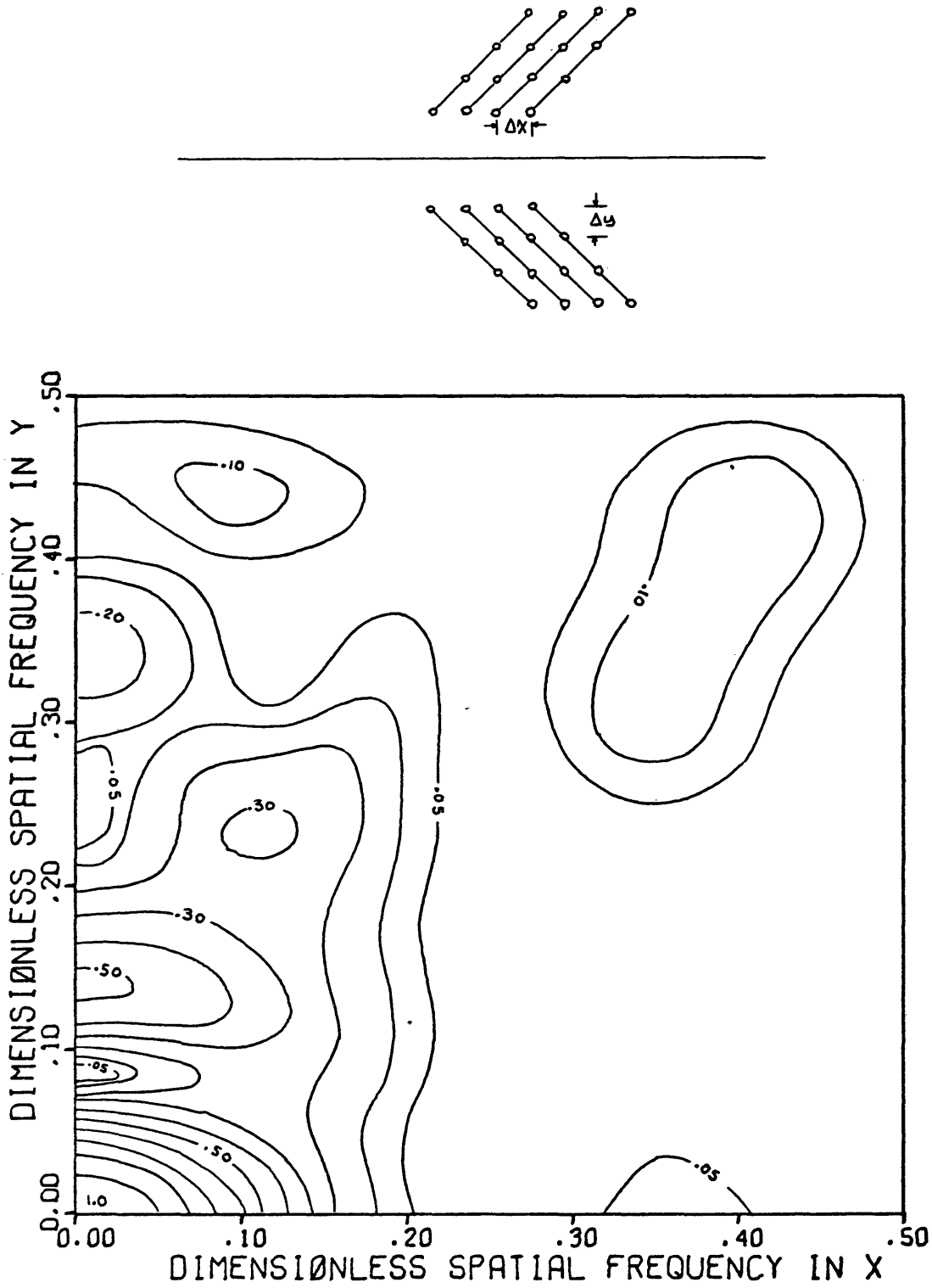


PLATE 10

32-geophone Array D

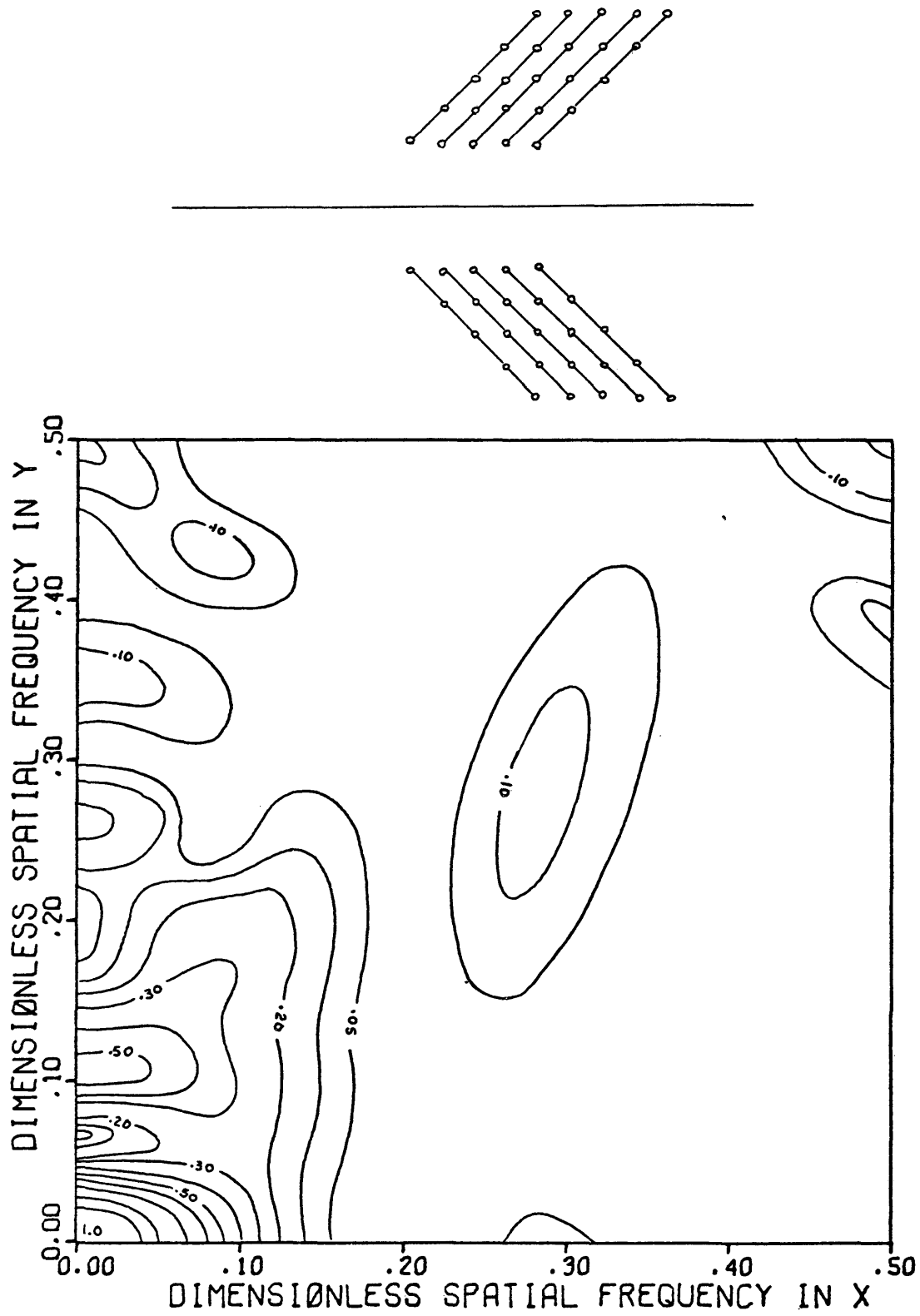


PLATE 11

50-geophone Array D

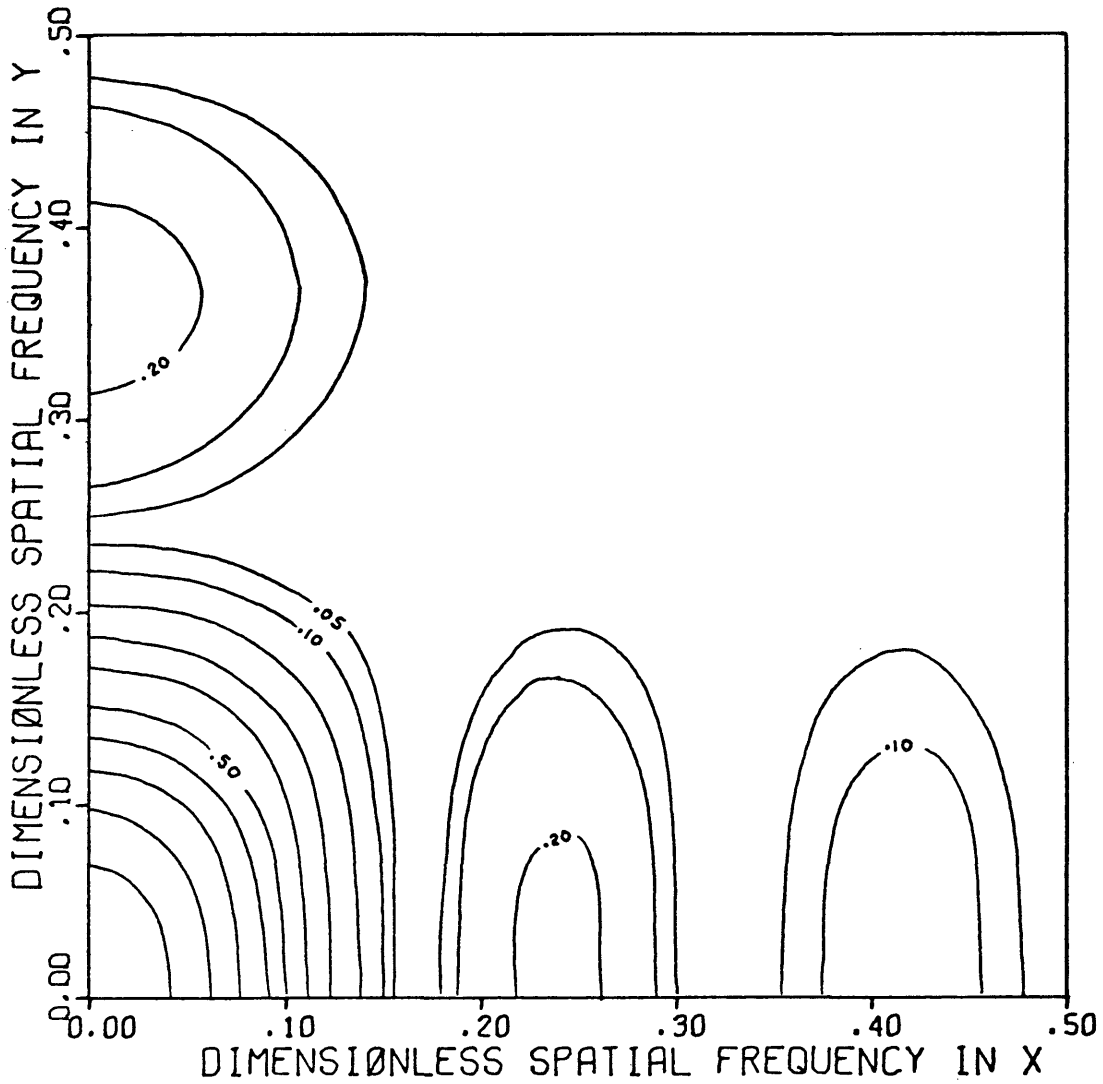
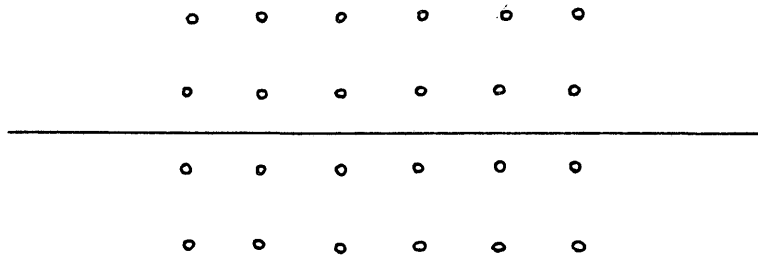


PLATE 12

24-geophone Rectangular Array

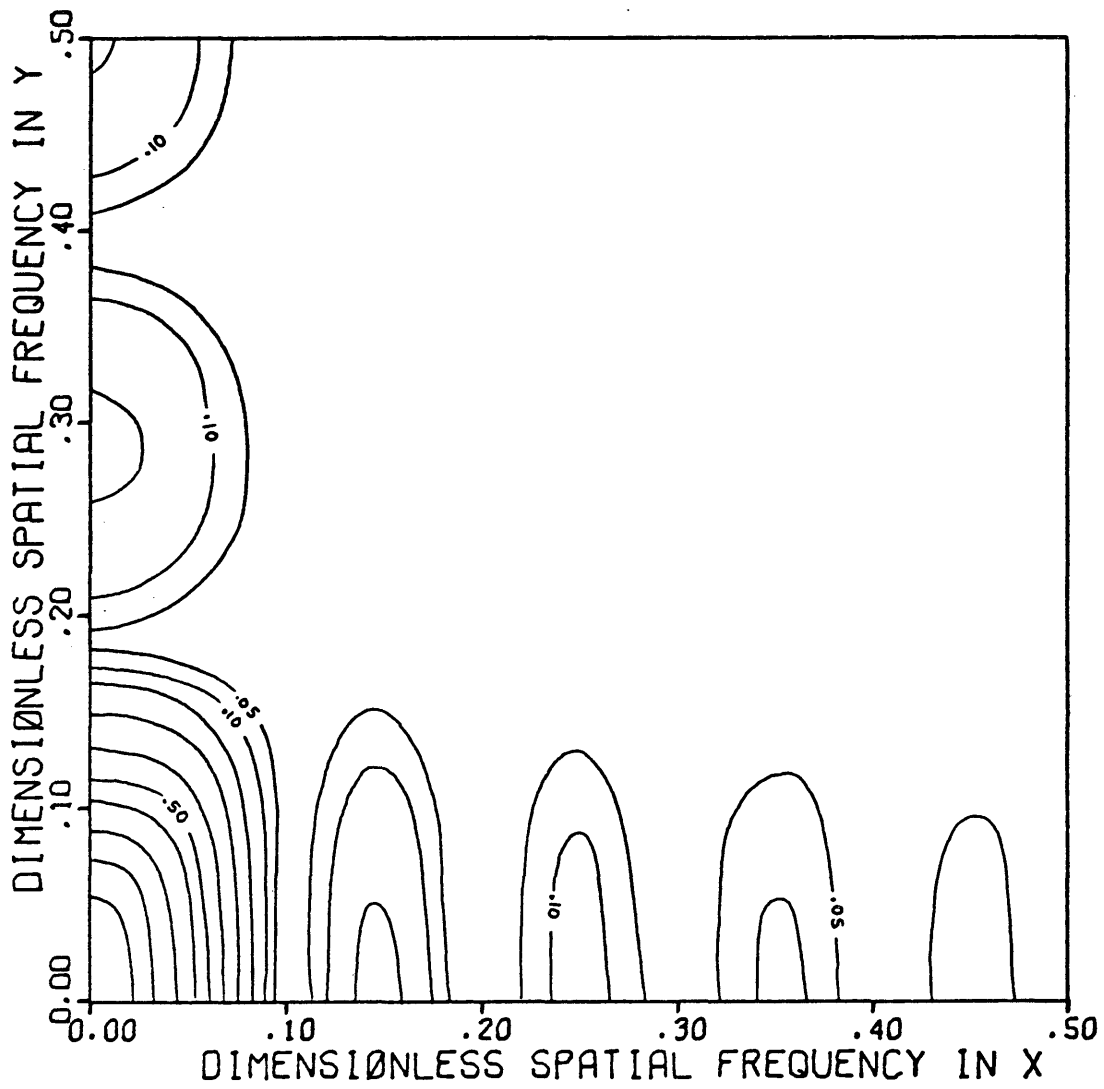
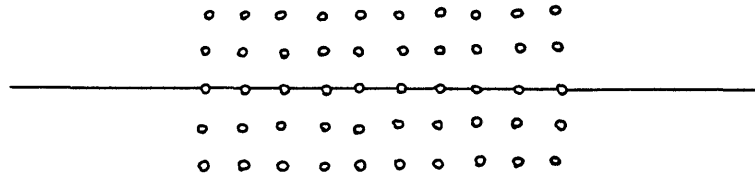


PLATE 13

50-geophone Rectangular Array

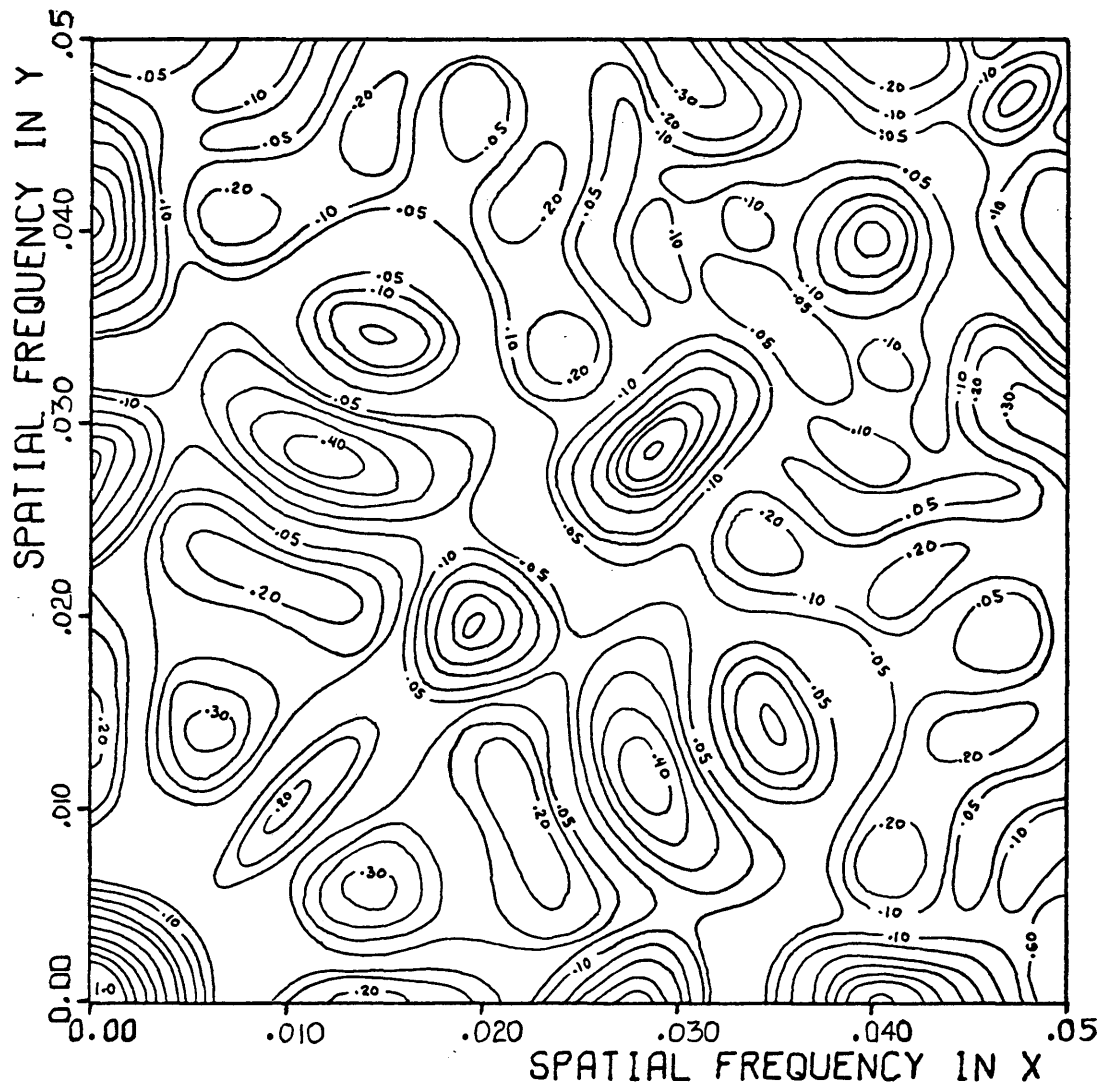
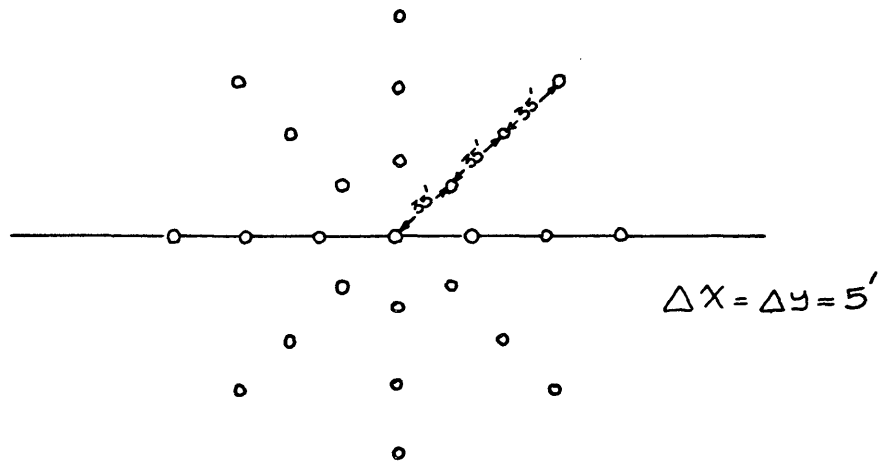


PLATE 14

25-geophone Circular Array

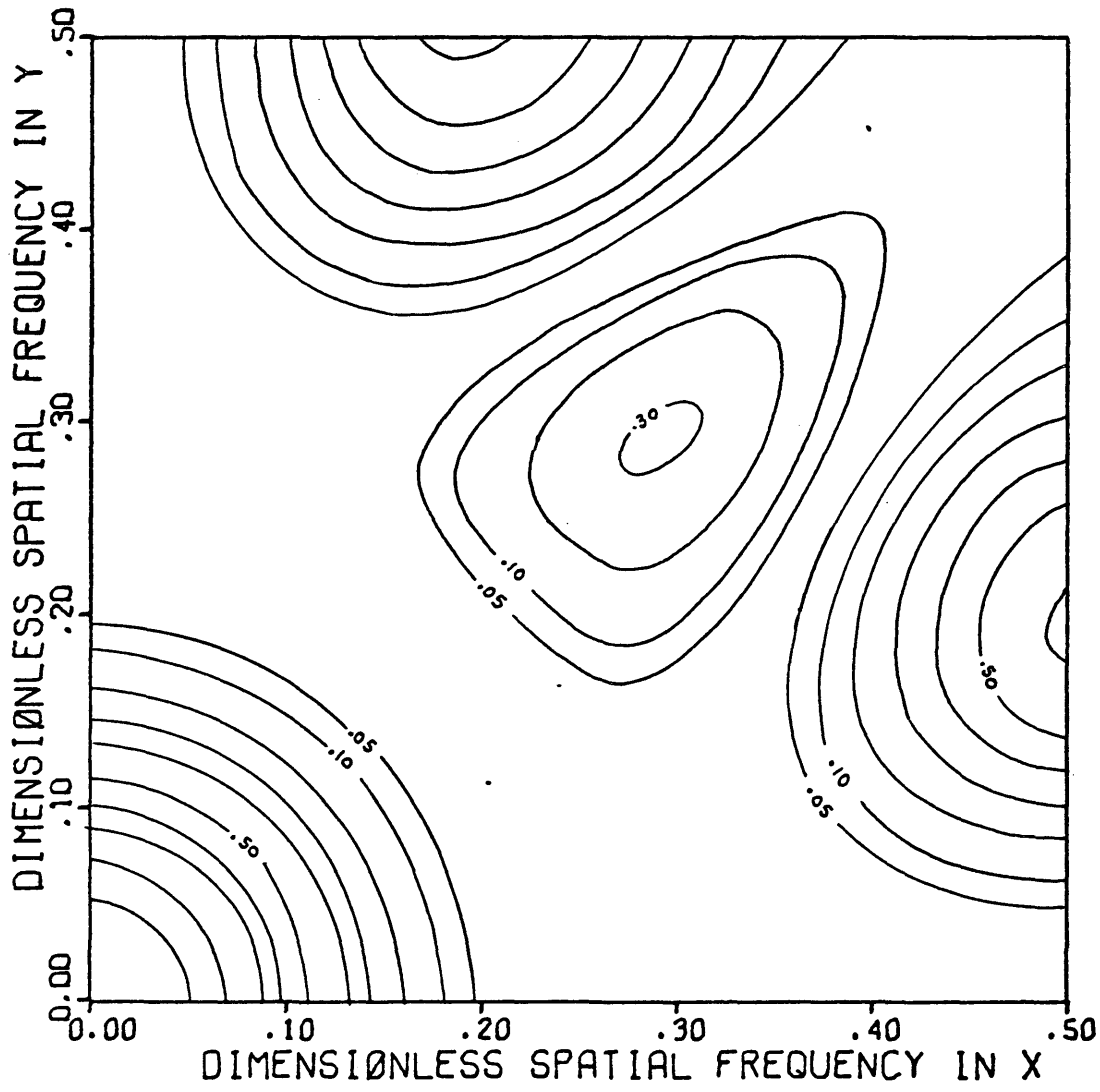
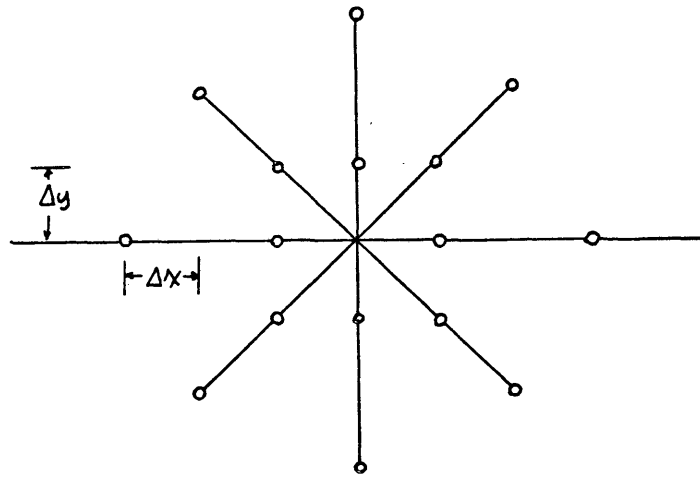


PLATE 15

16-geophone Star Array

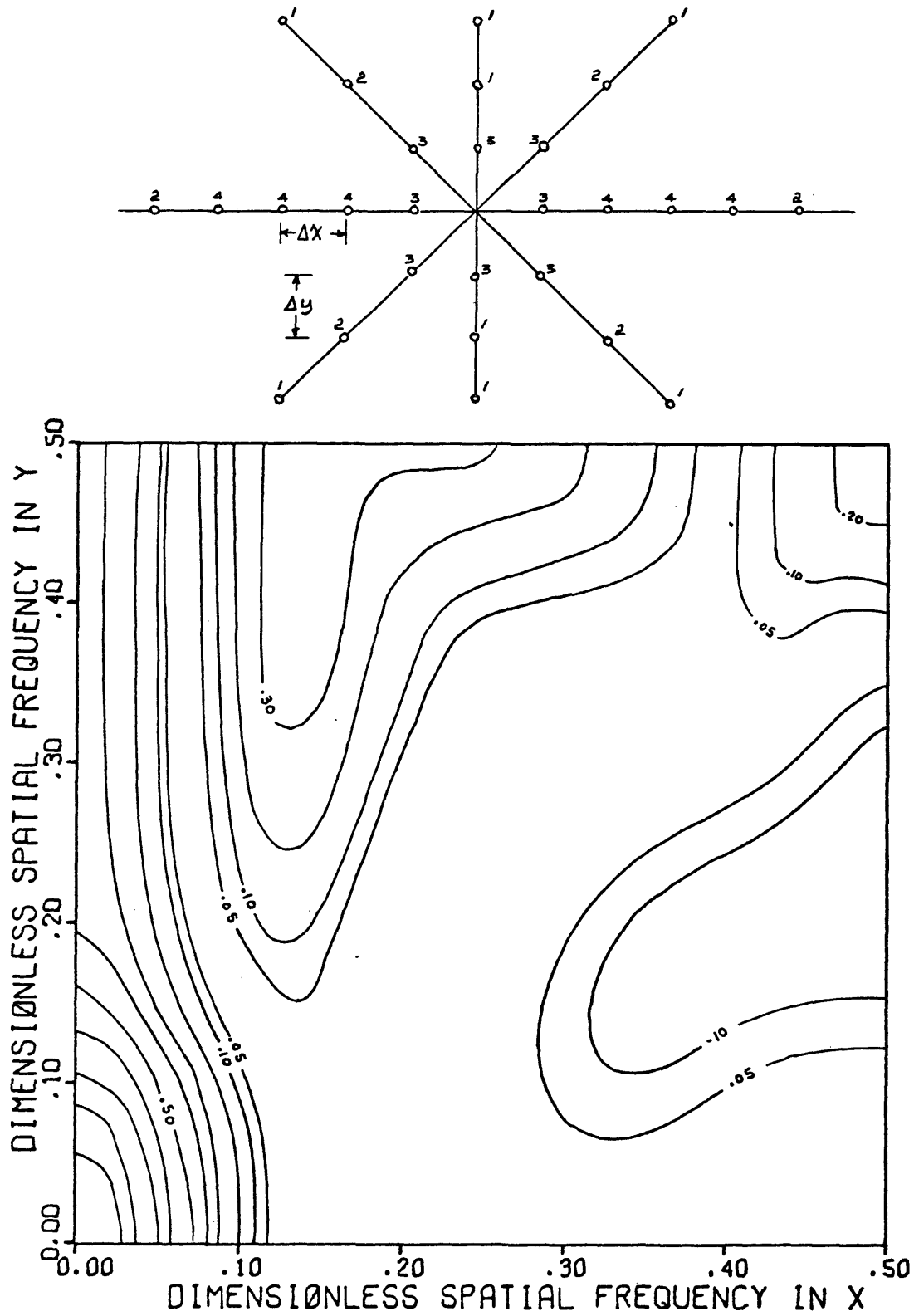


PLATE 16

Non-uniformly weighed 28-geophone Star Array. Numbers indicate the weights of individual geophones

CONCLUSIONS

The geophone array which was designed using truncated Sinc function approximation gives good rejection characteristics for the noise wave-numbers greater than the cut-off wave-number, and also shows zero or π phase shift in the direction in which the Sinc function extends.

Using the fundamental properties of two-dimensional Fourier transform, the amplitude response of an array can be computed from the amplitude response of its basic shape array. Amplitude response values of a deformed array can also be computed employing the method explained in the text.

The amplitude spectrum maps of arrays which have been presented should prove to be a great utility in designing geophone arrays in the field. The field geophysicist can also compute the amplitude spectrum of any array which can be obtained by rotating or deforming the basic array without need of computer. Response maps also give the perfor-

mance of the array for the wave-fronts arriving at the geophone at large angle of incidence and from arbitrary azimuths.

REFERENCES

- Bortfeld, R., Hurtgen, H., and Koppel, H., 1960, Direction shooting: Geophy. Prosp., v. 8, p. 534-561.
- Bracewell, R., 1965, The Fourier transform and its application: New York, McGraw-Hill, 381 p.
- Darby, E. K., and Davies, E. B., 1967, The analysis and design of two-dimensional filters for two-dimensional data: Geophy. Prosp., v. 15, p. 383-406.
- Gangi, A. F., and Disher, D., 1968, A space-time filter for seismic models: Geophysics, v. 33, p. 88-104.
- Graebner, R. J., 1960, Seismic data enhancement: Geophysics, v. 25, p. 283-310.
- Hadsell, F., 1968, An introduction to the theory of linear data processing: Colorado School of Mines, 221 p.
- Haubrich, A. R., 1968, Array design: Seismol. Soc. America, Bull., v. 58, p. 977-992.
- Holtzman, M., 1963, Chebyshev optimized geophone arrays: Geophysics, v. 28, p. 145-155.
- Jennings, W., 1965, First course in numerical methods: New York, MacMillan Co., 233 p.
- Lombardi, L. V., 1955, Notes on the use of multiple geophones: Geophysics, v. 26, p. 215-226.
- McCracken, D. D., 1968, A guide to Fortran iv programming: New York, John Wiley and Sons, Inc., 151 p.

- Papoulis, A., 1962, The Fourier integral and its applications: New York, McGraw-Hill, 311 p.
- _____, 1968, Systems and transforms with applications in optics: New York, McGraw-Hill, 474 p.
- Parr, J. O., and Mayne, H., 1955, A new method of pattern shooting: Geophysics, v. 20, p. 539-564.
- Savit, C. H., Brustad, J. T., and Sider, J., 1958, The move-out filter: Geophysics, v. 23, p. 1-25.
- Schelkunoff, S. A., 1943, A mathematical theory of linear array: Bell Sys. Tech. Jour., v. 22, p. 80-107.
- Smith, M. K., 1956, Noise analysis and multiple seismometer theory: Geophysics, v. 21, p. 337-360.
- Titchkosky, A. K., _____, Seismic deconvolution: 308 p. Privately printed.
- White, J. E., 1958, Transient behavior of patterns: Geophysics, v. 23, p. 26-43.